POLITECNICO DI TORINO

Department of Applied Science and Technology

PhD in Chemical Engineering
XXVII cycle (2012-2014)

THERMO-PHYSIOLOGICAL COMFORT MODELLING OF FABRICS AND GARMENTS

PhD student

Pezzin Alberto

Supervisors

Prof.ssa Ada Ferri

Prof. Silvio Sicardi

Second referee:

Ing. Paolo Caccavale

Coordinator:

Prof. Marco Vanni

Anno 2014

Contents

Abstract

Thermo-physiological comfort is a complex feeling affected by environment, by the metabolic rate and finally by the clothing.

It is crucial to understand the influence of the different variables, the environmental ones (such as air temperature and humidity), the metabolic ones (such as heat and moisture) and the clothing ones (such as air permeability, thermal resistance, etc..), and their relationships in order to design new garments that can satisfy the always more strictly requirements of technical textile in terms of comfort behaviour.

While the environmental conditions and metabolic rate are independent variables that should be analyzed but that cannot be modified, garments behaviour can be adjusted, using different materials, construction parameters, etc..., in order to give optimal thermo-physiological comfort.

In the last decades, more attention has been paid in the development of comfortable clothing for both technical and everyday use; for this reason, the interaction of garments with both the human body and the environment has been the subject of many studies.

This research work aims at analyzing the comfort properties of fabrics and to develop, using modelling techniques, a prediction method of comfort behaviour; four fabric properties, namely air permeability, thermal resistance, liquid and vapour transport through the fabric has been analyzed.

A fabric is a heterogeneous 3D ordered structure made of fibres, yarns and trapped air. In order to be able to predict its comfort properties it is necessary to predict its geometrical structure from its basic design parameters; this is the first stage for the development of any prediction method because comfort properties strongly depends on fabric structure. In this work a realistic 3D model of fabrics has been realized starting from their design parameters in order to lay the foundations for a fully predictive design method.

The second stage of this research work has been focused on the simulation of the fabrics comfort properties, for different fabrics structures and compositions, and their validation with experimental values.

Air permeability, that represents the resistance to air flowing through the fabric, is one of the most important parameters that influence comfort properties, because it influences both the vapour and moisture transport and thermal properties. The simulations have shown that it is possible to predict, with a good approximation, air permeability behaviour of different fabrics.

Thermal resistance has been investigated using a simplified geometry of textile fabrics; in this case there is a quite good approximation of the simulated values due to this simplified geometry. For thermal properties modelling not only the comparison with experimental tests has been done but also some simulations that better represents a real case, in which fabric is not pressed between the measuring heads but where its distance from the skin can vary from contact to some millimetres.

Also vapour transport and adsorption process have been investigated in order to analyze the behaviour of different fibres and for different temperature and relative humidity conditions. When the human body is under low physical activities the air layer between skin and fabric can reach temperature in the range of 30°C to 40°C and relative humidity in the range of 60% to 90%; in these cases the prediction of the adsorption mechanism, that is an exothermic process, has to be taken into account especially for natural fibres that have high values of differential heat of sorption.

Last but not least the liquid transport has been analyzed; in fact the presence of liquid is very important during high intensity physical activities and has to be taken into account because it highly influences the thermal properties of any fabric. Not only thermal properties are influenced but liquid also causes a wetness sensation that is very uncomfortable; for these reasons the liquid should be transported to the outer fabric surface as quickly as possible.

Finally a case-study, represented by a 3D model of a back protector, is presented; using the experimental data measured in the climatic chamber at the Advanced Technology Textile Laboratory in Biella, some thermal simulations has been carried out.

The research aims to develop a simulation method that starting from the basically constructive parameters of fibres, yarns and fabrics used to create any 3D fabric geometries leads to a fully predictive simulation method that allow to reduce the costs for the development of new high performance fabrics.

1 - The human comfort

1.1 Introduction

Human comfort is "freedom from pain, freedom from discomfort. It is a neutral state." [1] and it is "a state of physiological, psychological and physical harmony between a human being and the environment." [2]

Comfort is a subjective feeling, depending by the external ambient, by the clothing and by the physical activity.

Comfort can be divided into two main types, psychological and physiological comfort. Psychological comfort refers to the needing of each person to wear specific garments in terms of colors and design features in order to make them feeling well while physiological comfort is mainly affected by the thermal balance, namely the relationship between the body heat production and the losses.

Human comfort is influenced by three main parameters:

➢ The external ambient
➢ The human body
➢ The clothing

1.2 - The external ambient

At the top of the earth atmosphere the sun radiates an energy of approximately 1370 W/m^2 and the human life depends from this energy.

This energy is radiated in every place of earth and it creates the difference types of environments that exist; every person had to interact with this wide range of conditions and it is necessary to be able to efficiently react to these different conditions.

For the environment analysis there are four main parameters that can be considered [3] :

➢ Air temperature
➢ Radiant temperature

➢ Humidity
➢ Air movements

1.2.1 - Air temperature

The temperature of a human body is highly affected by the temperature of the fluids or solids surrounding it. Normally a human body is surrounded by clothing and then typically by air.

The air temperature (t_a) can be defined as the temperature of the air surrounding the human body which is representative of that aspect of the surroundings which determines heat flow between the human body and the air. [3]

The air temperature is not constant and for the analysis of the comfort we cannot use both the temperature of the air at a great distance from the body because it do not represent correctly the heat flow between the body and the environment even and the air temperature very close to the body because it is influenced by the boundary layer at the air-body interface.

1.2.2 - Radiant temperature

In addition to the air temperature it is necessary to take into account also the radiant temperature that represent the heat flow exchanged between different bodies due to their different temperature. The thermal radiation is a part of the electromagnetic spectrum that includes X-rays, light and radio waves. The thermal radiation can be simply related to the light that pervade all the environments with can be reflected, absorbed and refracted; every person moving in an environment cause a variation in reflection, refraction and absorption and so in every point of space there is a unique thermal radiation. In order to take into account the effect of the thermal radiation a radiant temperature has been defined by McIntyre [4] as "the temperature of a black-body source that would give the same value of some measured quantity of the radiation field as exists in reality".

For practical uses two different radiant temperature has been defined to summarize the heat exchange between the human body and the environment: the mean radiant temperature and the plane radiant temperature.

The mean radiant temperature (t_r) is defined as "the temperature of a uniform enclosure with which a small black sphere at the test point would have the same radiation exchange as it does with real environment" [3]; this definition implies the calculation of an average value in the three dimension because using a sphere it has no relevancy of their orientation in the environment.

In case of a non-spheroidal shape such as a human body it is possible to use the effective mean radiant temperature that is defined as "the temperature of an uniform enclosure with which the test surface would have the same radiation exchange as it does

with the real environments" [3]; this value depends upon the orientation of the object in the surroundings.

The plane radiant temperature (t_{pr}) is define by the ISO 7726 as "the uniform temperature of an enclosure where the radiance on one side of a small plane element is the same as in the non-uniform actual environment". This temperature takes into account the exchange in one direction and so it is hardly influenced by the orientation of the body.

The mean radiant temperature for a standing man can be estimated, according to the ISO 7726, using the plane radiant temperature measured in six different orientation using Eq.1.1.

$$t_r = \frac{0.08\left(t_{pr1} + t_{pr2}\right) + 0.23\left(t_{pr3} + t_{pr4}\right) + 0.35\left(t_{pr5} + t_{pr6}\right)}{2\left(0.08 + 0.23 + 0.35\right)} \qquad [1.1]$$

where:
t_{pr1}: plane radiant temperature in direction up
t_{pr2}: plane radiant temperature in direction down
t_{pr3}: plane radiant temperature in direction right
t_{pr4}: plane radiant temperature in direction left
t_{pr5}: plane radiant temperature in direction front
t_{pr6}: plane radiant temperature in direction back

Radiant temperatures can be used both for indoor and for external environments.
For outdoor environments the radiation is given by the sun and the radiant heat depends from the level of radiation, the wavelength of the radiation, the direction of the radiation received by the body and the body and posture orientation.

The radiation of sun at the earth ground has a maximum value of about 1000 W/m2 as some part of this energy is scattered and absorbed by the atmosphere due to cloud, pollution, etc...; the radiation value depends on the location, day of the year, weathering conditions and hour of the day.

For the thermal analysis of a human body there are six radiation terms that are relevant [5]: three solar radiation terms (direct, diffuse and reflected), two thermal radiation terms (sky and ground) and the thermal radiation emitted from the body, as it can be seen in Fig.1.1 [6].
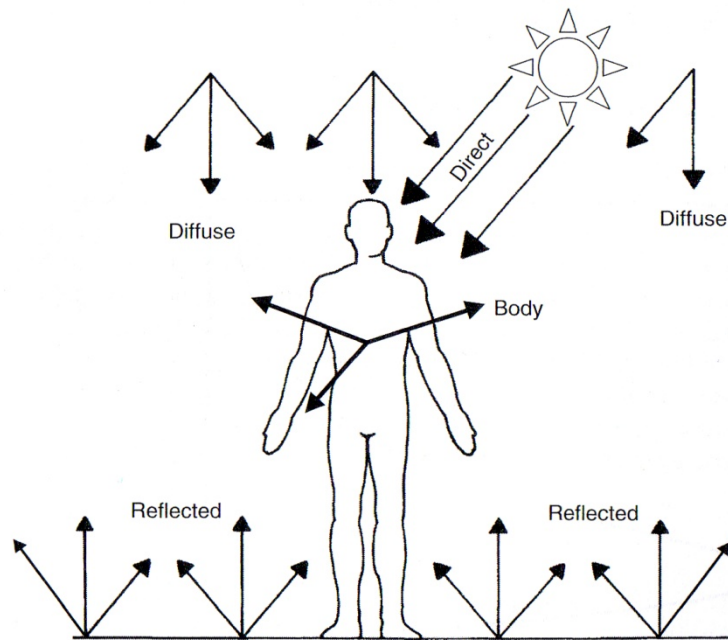
Figure 1.1 - The impact of direct, diffuse and reflected solar radiation

1.2.3 - Air velocity

Human body is often surrounded by air and for this reason air movements, that are not constant in time, space and direction, are of relevant importance to determine the heat exchange between the body and the environment.
For simplicity a scalar value, the air speed, can be considered to be the mean air velocity intensity evaluated over an exposure time and integrated over all directions.
Due to the relevant effects of air velocity, ISO 7730 suggest that both the mean air velocity value and its standard deviation had to be considered.

1.2.4 - Humidity

When a liquid, water or sweat, is heated by the human body is evaporated and it leaves the body surface and is lost in the environment; this process had as consequence an heat flow from the body, that is cooled, to the environment.
The driving force for this mass transfer process is the difference in the concentration of water between the air near the skin surface and the environment; for convenience this driving force is defined as the difference in the partial vapour pressures between that measured at the skin surface and that in the environment.
The two commonly forms to express air humidity are the relative humidity and the partial vapour pressure.

Relative humidity (Φ) is the ratio between the partial pressure of water vapour (P_a) and the saturated water vapour pressure (P_{sa})

$$\Phi = \frac{P_a}{P_{sa}} \qquad [1.2]$$

The partial pressure of water vapour depends from the temperature of the air: increasing the air temperature the maximum quantity of vapour that can be hold in the air increase. The saturated vapour pressure can be calculated using the Antoine's equation (Eq.1.3):

$$P_{sa} = \exp\left(18.956 - \frac{4030.18}{T + 235}\right) \qquad [1.3]$$

where T is the air temperature expressed in °C.

1.3 - The human body

The optimal human body internal temperature should be around 37 °C and to achieve this result should have an heat balance between the body and the environment.
There is no steady state conditions because internal and external temperatures will vary in time but there is a dynamic balance between the heat flow into the body and the internal heat generation and the heat outputs from the body. The heat balance equation for the human body includes three types of terms:
  ➢ The heat generation inside the body
  ➢ The heat transfer between the body and the environment
  ➢ The heat storage
For the body in heat balance the rate of heat storage is zero.

The balance equation can be written as:

$$\left(\dot{M} - \dot{W}\right) = \left(\dot{E} + \dot{R} + \dot{C} + \dot{K}\right) + \dot{S} \qquad [1.4]$$

where (all unit are in [W/m^2]):
$\dot{M}$: metabolic rate of the body
$\dot{W}$: mechanical work
$\dot{E}$: heat transfer due to evaporation
$\dot{R}$: heat transfer due to radiation
$\dot{C}$: heat transfer due to convection
$\dot{K}$: heat transfer due to conduction
$\dot{S}$: heat storage

In this equation $(\dot{M} - \dot{W})$ is a term always positive and represents the heat released by the body.

The use of W/m^2 unit is due to the necessity to standardize the energy balance over persons of different sizes; in order to calculate the energy balance for a human body it can be use the simplified equation, written by Dubois [7], to estimate the total body surface area.

$$A_D = 0.202 * W^{0.425} * H^{0.725} \qquad [1.5]$$

where:

A_D: Dubois surface area [m^2]
W: weight of body [kg]
H: height of body [m]

In order to allow the calculation of the heat balance equation it is necessary to determine the heat production and exchange for the human body; this can be done writing the heat balance equation using terms that can be measured or estimated.

Fanger [8] proposes this heat balance equation:

$$\dot{H} - \dot{E}_{dif} - \dot{E}_{sw} - \dot{E}_{res} - \dot{C}_{res} = \dot{R} + \dot{C} \qquad [1.6]$$

where (all unit are in [W/m^2]):

$\dot{H}$: metabolic heat production
$\dot{E}_{dif}$: heat loss by vapour diffusion through skin
$\dot{E}_{sw}$: heat loss by evaporation of sweat
$\dot{E}_{res}$: latent respiration heat loss
$\dot{C}_{res}$: dry respiration heat loss
$\dot{C}$: heat transfer due to convection
$\dot{R}$: heat transfer due to radiation

In this equation heat transfer by conduction is assumed to be negligible.

ASHRAE [9] gives the following equation of heat balance:

$$\dot{M} - \dot{W} = \dot{Q}_{sk} + \dot{Q}_{res} = \left(\dot{C} + \dot{R} + \dot{E}_{sk} \right) + \left(\dot{C}_{res} + \dot{E}_{res} \right) \qquad [1.7]$$

where (all unit are in [W/m^2]):

$\dot{M}$: metabolic rate of the body

$\dot{W}$: mechanical work

$\dot{Q}_{sk}$: total rate of heat loss from the skin

$\dot{Q}_{res}$: total rate of heat loss through respiration

$\dot{C}$: heat transfer due to convection

$\dot{R}$: heat transfer due to radiation

$\dot{E}_{sk}$: heat loss by evaporation from the skin

$\dot{E}_{res}$: evaporative heat loss from respiration

$\dot{C}_{res}$: convective heat loss from respiration

The rate of evaporative heat loss from the skin can be written as:

$$\dot{E}_{sk} = \dot{E}_{rsw} + \dot{E}_{dif} \qquad [1.8]$$

where (all unit are in [W/m^2]):

$\dot{E}_{rsw}$: evaporative heat loss from the skin through sweating

$\dot{E}_{dif}$: evaporative heat loss from the skin through moisture diffusion

In Eq.1.7 there are three main terms:
- ➢ Heat production within the body
- ➢ Heat loss at the skin
- ➢ Heat loss due to respiration

1.3.1- Heat production within the body

This terms is related to the physical activity of the person and depends from the metabolic heat rate production and from the mechanical work that can vary from about zero to a maximum of 25% of the metabolic rate.

Human body requires an amount of energy for use in membrane transport, chemical reactions and mechanical work; this energy is supplied by ATP (adenosine triphosphate) that is made using glucose obtained from food and oxygen obtained from respiration.

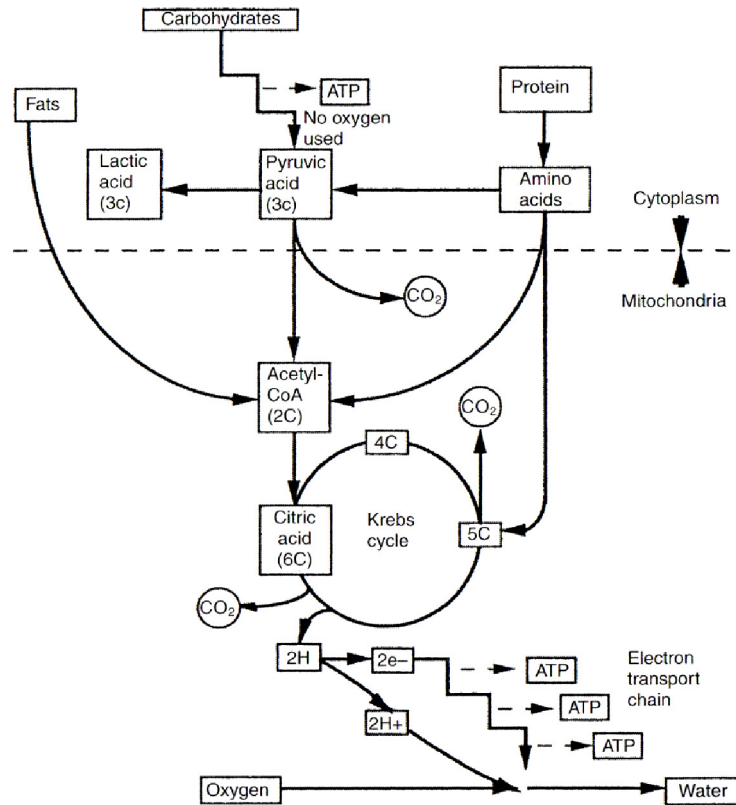The process that leads to the production our this energy is shown in Fig.1.2 [9].

Figure 1.1 - ATP production process

Carbohydrates are converted into glucose, proteins into amino acids and fats into fatty acids in the gastrointestinal apparatus and then they are transported with oxygen into the cytoplasm of the cell; here there are other transformations that convert glucose into pyruvic acid and fatty acids and amino acids into acetoacetic acid. These chemicals reach the mitochondria, the power plant of the cell, where they are convert into ATP, carbon dioxide and water in the Krebs cycle.

Approximately 95% of the ATP produced by human body is formed inside the mitochondria.

Most of the energy produced in this process is released as heat that is transported in all the body through the bloodstream; the integration of the heat produced is called total metabolic heat production of the body ($\dot{H}$).

Metabolic heat production can be written as the difference between the total energy produced ($\dot{M}$) and the total work ($\dot{W}$).

$$\dot{H} = \dot{M} + \dot{W} \qquad [1.9]$$

Metabolic heat production is the fifth parameters that as to be taken into account in the analysis of comfort together with the external ambient parameters analyzed in Chapter 1.2.

Metabolic heat production can be measured using a calorimetric method while the metabolic rate can be estimated using indirect calorimetry; for practical uses the metabolic heat production can be estimated using tables that takes into account different physical activities. These values are valid for a man with a body surface area of about 1.84 m^2 and a weight around 65 kg; sometimes instead of using W/m^2 data are shown in Met, a unit corresponding to 58.15 W/m^2, that represent the metabolic rate of a seated person at rest.

The external work can be calculated by multiplying the force applied to do something by the distance moved in the direction of the force; for many tasks it is very difficult to calculate the external work.

The mechanical efficiency (η) doing something can be calculated as:

$$\eta = \frac{\dot{W}}{\dot{M}} \qquad [1.10]$$

Maximum value of mechanical efficiency is around 25% but for many tasks is close to zero.

Table 1.1 reports some values of the metabolic rate at different work intensities, table 1.2 reports some values of the metabolic rate for different occupation and table 1.3 shows some metabolic rate values for basic activities. [3]

General description	Metabolic rate [W/m^2]
Resting	*65*
Low	*100*
Moderate	*165*
High	*230*
Very high	*290*

Table 1.1 - Estimates of metabolic rate based on different work intensities

Occupation	Metabolic rate [W/m^2]
Bricklayer	*110-160*
Painter	*100-130*
Foundry worker	*140-240*
Tractor driver	*85-110*
Secretary	*70-85*

Table 1.2 - Estimates of metabolic rate based on different occupations

Basic activity	Metabolic rate [W/m^2]
Lying	*45*
Sitting	*58*
Standing	*65*
Walking on level even path at 2 km/h	*110*
Walking on level even path at 5 km/h	*200*
Going upstairs, 80 stairs per minute	*440*
Transporting a 10 kg load on the level at 4 km/h	*185*

Table 1.3 - Estimates of metabolic rate for basic activities

1.4 - The clothing

The third main parameter that as effect on the human comfort is the thermal behaviour of clothing; this is a complex behaviour that has been studied from many researchers. There are many factors that can influence the thermal behaviour of clothing such as dry thermal insulation, air permeability, water vapour permeability, moisture adsorption, etc...

1.4.1 - One parameter model: dry thermal insulation

Dry thermal insulation is one of the most important parameters in the analysis of the clothing behaviour; the most simple model is composed by a heated body with a layer of insulation clothing as shown in Fig. 1.3 [3]
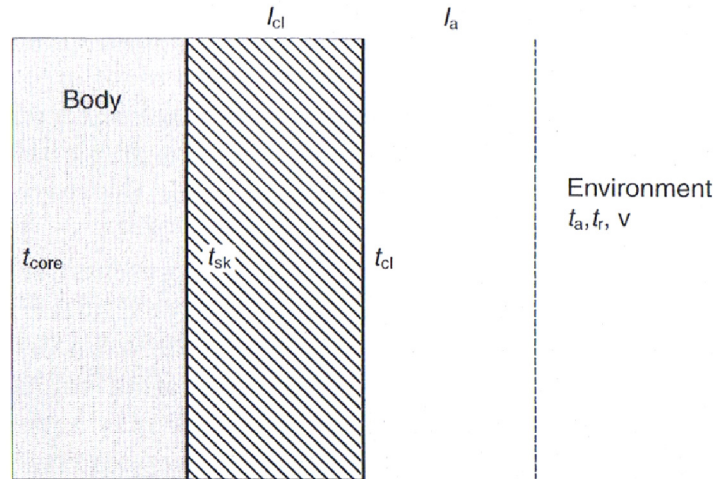
Figure 1.2 - Thermal model with a layer of clothing insulation

where:

t_{core}: mean core temperature

t_{sk}: mean skin temperature

t_{cl}: surface temperature of the clothed body

t_a: air temperature

t_r: mean radiant temperature

v: air velocity

I_{cl}: intrinsic clothing insulation

I_a: thermal resistance of the environment

Metabolic heat is produced in all the human body and it is transferred to the skin layer thanks to the thermo-regulatory system; in order to maintain an internal temperature around 37°C blood flows in the skin layer, thanks to the vasodilatation mechanism, to release heat to the environment. When metabolic heat increase the bloodstream is not enough to drain all the heat produced so the skin surface is moistened with sweat so that the latent heat of vaporization can be lost through evaporation.

At the skin surface is placed the clothing layer that can be seen as a resistance to the heat flow from the body to the environment; this layer can be simplified using an intrinsic clothing insulation value (I_{cl}) that is the reciprocal of the clothing conductivity.

When heat reach the clothing surface it meets the air layer in which the heat transfer depends from the convection and the radiation mechanism.

For a nude body the thermal resistance of the environment is given by [3]:

$$I_a = \frac{1}{h} \qquad [1.11]$$

and

$$h = h_r + h_c \qquad [1.12]$$

where
h_r: radiative heat transfer coefficient
h_c: convective heat transfer coefficient

In case of a clothed body the surface area involved in the heat transfer mechanism is increased due to the clothing layer and this is related to the thickness of the clothing.
In order to take into account this effect it is possible to add an additional term into Eq. 1.11.

$$I_a\left(clothed\right) = \frac{1}{f_{cl}h} \qquad [1.13]$$

where f_{cl} is the ratio between the clothed surface area of the body and the nude surface area.
It is not so easy to determines this value and different methods can be find in literature; some are based on photographic techniques, such as that proposed by Jones [10], while others are estimated from the intrinsic clothing value, such as that proposed by McCullough [11] that gives an approximation of this coefficient for indoor ensembles.

In order to combine the effect of the clothing layer and the air layer it is possible to define the total clothing insulation value using the equation proposed by Parson [12]:

$$I_t = I_{cl} + I_a\left(clothed\right) \qquad [1.14]$$

In order to calculate the intrinsic clothing insulation value for a clothing ensemble the following equation, proposed in the ISO 9920 (1995), can be used

$$I_{cl} = \sum I_{clu,i} \qquad [1.15]$$

where
$I_{clu,i}$ = effective insulation for garment i

In table 1.4 are reported typical thermal insulation values for different garments [3].

Garment description	Thermal insulation Iclu [m2*°C/W]
Underwear	
Panties	0.005
Underpants with long legs	0.016
Singlet	0.006
T-shirt	0.014
Shirt with long sleeves	0.019
Panties and bra	0.005
Shirts/blouses	
Short sleeves	0.023
Lightweight, long sleeves	0.031
Normal, long sleeves	0.039
Flannel shirt, long sleeves	0.047
Lightweight blouse, long sleeves	0.023
Trousers	
Shorts	0.009
Lightweight	0.031
Normal	0.039
Flannel	0.043
Dresses/skirts	
Light skirt (summer)	0.023
Heavy dress (winter)	0.039
Light dress, short sleeves	0.031
Winter dress, long sleeves	0.062
Boiler suit	0.085
Sweaters	
Sleeveless vest	0.019
Thin sweater	0.031
Sweater	0.043
Thick sweater	0.054

Jackets	
Light summer jacket	0.039
Jacket	0.054
Smock	0.047
High insulative, fibre-pelt	
Boiler suit	0.140
Trousers	0.054
Jacket	0.062
Vest	0.031
Outdoor clothing	
Coat	0.093
Down jacket	0.085
Parka	0.109
Fibre-pelt overalls	0.085
Sundries	
Socks	0.003
Thick ankle socks	0.008
Thick long socks	0.016
Nylon stockings	0.005
Shoes (thin soled)	0.003
Shoes (thick soled)	0.006
Boots	0.016
Gloves	0.008

Table 1.4 - Thermal insulation values for different garments

1.4.2 - Two parameter model: dry thermal insulation and moisture transfer

The one parameter model describe in cap. 1.4.1 does not take into account the heat that can be transfer between the body and the environment due to the evaporation of sweat. In figure 1.4 a schematic representation of this model is reported [3].
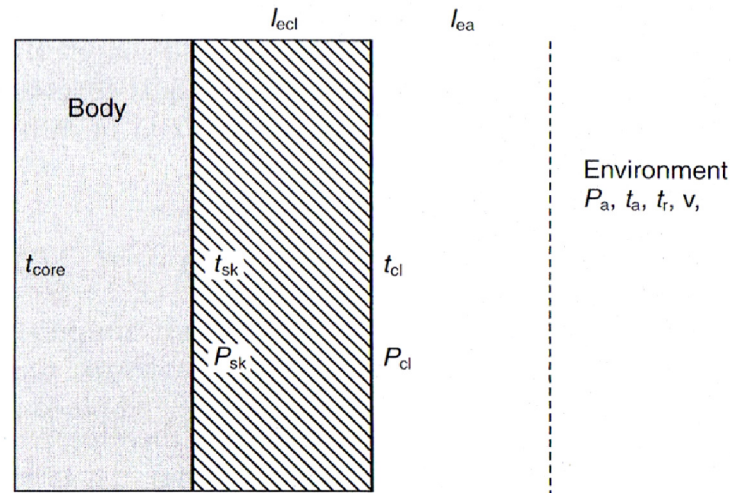
Figure 1.3 - Two parameters model representation

where:

t_{core}: mean core temperature

t_{sk}: mean skin temperature

t_{cl}: surface temperature of the clothed body

t_a: air temperature

t_r: mean radiant temperature

v: air velocity

P_{sk}: partial vapour pressure at the skin surface

P_{cl}: partial vapour pressure at the clothing surface

P_a: partial pressure of water vapour in air

I_{ecl}: intrinsic evaporative resistance

I_{ea}: vapour transfer resistance of the air layer

In presence of sweat at the skin surface it evaporates and it is transported through the clothing layer to the environment; is the difference between the partial pressure that can be considered as driving force for the heat transport process.

The resistance of clothing to the vapour transfer is called intrinsic evaporative resistance (I_{ecl}).

At the skin surface the partial pressure is assumed to be the saturated vapour pressure that can be calculated from Eq. 1.3.

Vapour transfer to the clothing surface reaches the air layer that has its resistance to the vapour transfer (I_{ea}) that depends from the evaporative heat transfer coefficient (h_e).

The evaporative heat transfer coefficient is related to the convective heat transfer coefficient (h_c) by the Lewis number, using the Eq. 1.16.

$$Le = \frac{h_e}{h_c} \qquad [1.16]$$

This relationship is independent from the size and shape of the body and from air speed or temperature; it depends only from the physical properties of the gas medium.

Since the Lewis number at sea level and for air is around 16.5 MPa^{-1} the resistance to the vapour transfer coefficient can be written as:

$$I_{ea} = \frac{1}{h_e} = \frac{1}{16.5 \cdot h_c} \qquad [1.17]$$

1.4.3 - More complex model

The two parameters model do not represents the real behaviour of the clothing assembly because sweat do not evaporate only at the skin surface.
The first improvement to this model is to consider wicking of liquid through clothing materials with the evaporation occurring also inside the clothing layer; this model, proposed by Kerslake [13], is shown in figure 1.5.
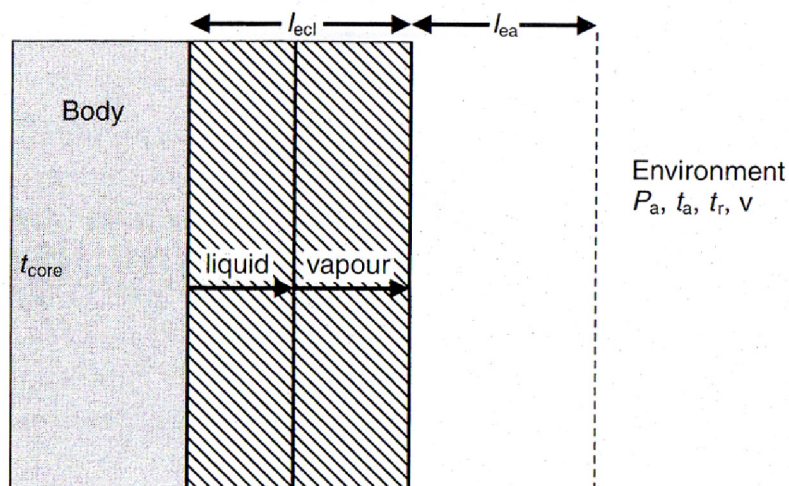
Figure 1.5 - Kerslake model with wicking

Another extension to the two parameters model is to take into account the clothing ventilation since heat and vapour can be lost through the macro pores of the clothing surface and for direct penetration of air through the clothing.
If clothing ventilation is considered to be negligible the predicted value of clothing insulation will be higher than the real one for cold environments and for hot environments the predicted evaporative heat loss will be smaller than the real one.
The last things that as to be considered is that the clothing layer is not all in contact with the skin surface but there is a layer of air trapped between the skin surface and the clothing.

A four layer model was presented by Lotens [14,15] and it takes into account the effects of wind penetration through openings, clothing ventilation and air trapped between the layer; a schematic representation of this model is shown in figure 1.6.
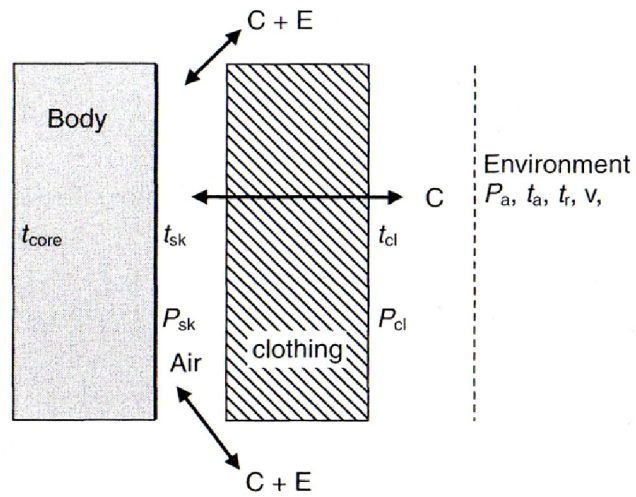
Figure 1.6 - Lotens model scheme

2 - Textile fabrics

2.1 Introduction

As shown in Cap.1 clothing is one of the three most important parameters that affect the human comfort.
Comfort properties of clothing depends mainly from their fabrics properties such as fiber material, yarn properties and fabric structure.

2.2 - Fiber material

Fibre material is the first parameter to be considered in the evaluation of the fabric properties because it influences the final value of thermal conductivity, heat capacity and moisture adsorption.
Textile fibre can be divided into two main categories, natural and chemical fibre as shown in Fig. 2.1.
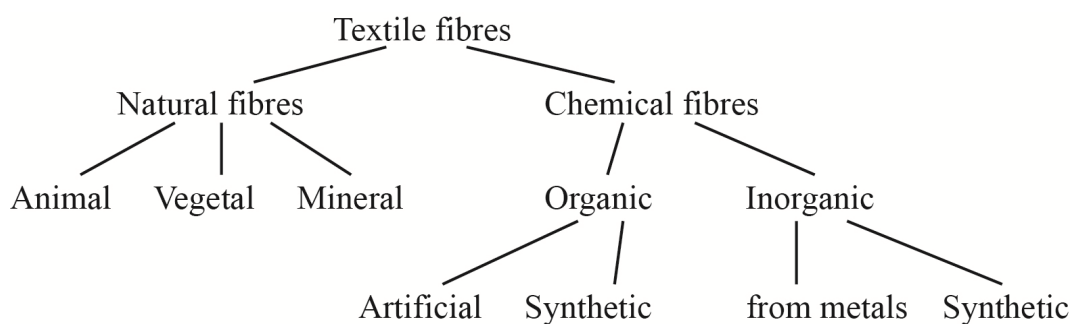
Figure 2.1 - Textile fibres classification

The most common natural fibres are reported in Fig. 2.2.
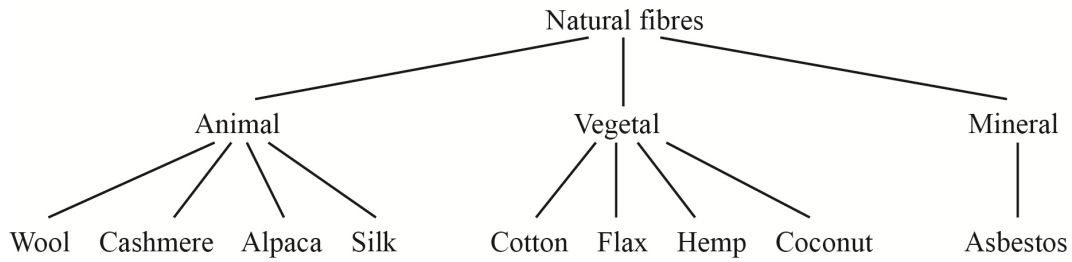
Figure 2.2 - Typical natural fibres

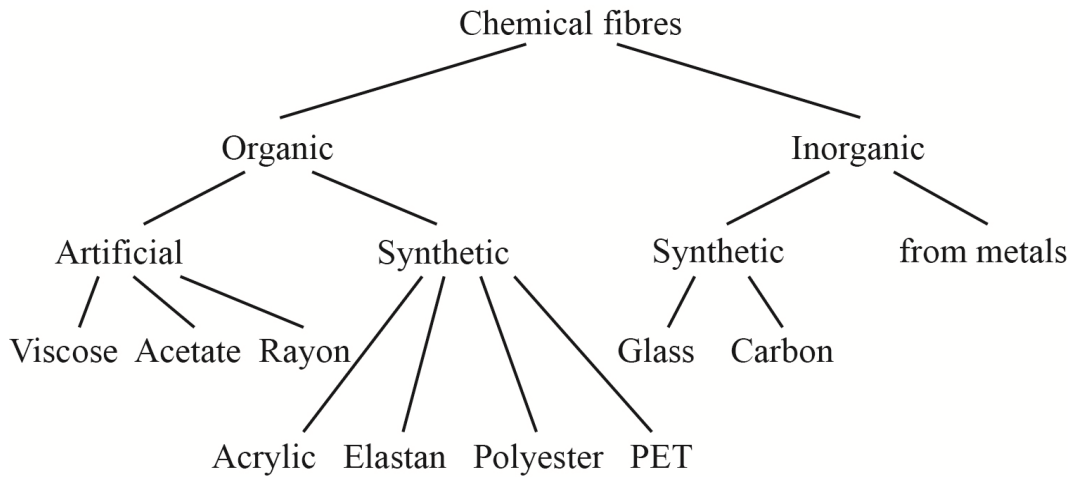The most common chemical fibres are shown in Fig. 2.3.

Figure 2.3 - Typical chemical fibres

For comfort properties evaluation some properties of the fibres are relevant, namely thermal conductivity, density, specific heat and moisture adsorption; these properties are reported, for most common fibres, in the following tables [16].

Fibre material	Thermal conductivity (*k*) [W/(m*K)]
Wool	*0.165*
Cotton	*0.243*
Flax	*0.344*
Silk	*0.118*
Rayon	*0.237*
Acrylic	*0.172*
Polypropylene	*0.111*
Polyester	*0.127*
Nylon	*0.171*

Table 2.1 - Thermal conductivity values for different fibres

Fibre material	Dry density (ρ) [W/(m*K)]
Wool	*1300*
Cotton	*1550*
Flax	*1410*
Silk	*1340*
Rayon	*1520*
Acrylic	*1190*
Polypropylene	*910*
Polyester	*1390*
Nylon	*1140*

Table 2.2 - Dry density values for different fibres

Fibre material	Specific heat (*Cp*) [J/(kg*K)]
Wool	*1360*
Cotton	*1220-1350*
Flax	*1280-1400*
Silk	*1380*
Rayon	*1350-1590*
Acrylic	*1400-1500*
Polypropylene	*1925*
Polyester	*1030*
Nylon	*1450*

Table 2.3 - Specific heat values for different fibres

Moisture regain properties are highly dependent from the relative humidity of air; moisture regain curves at 20°C are shown in Fig. 2.4 [16].
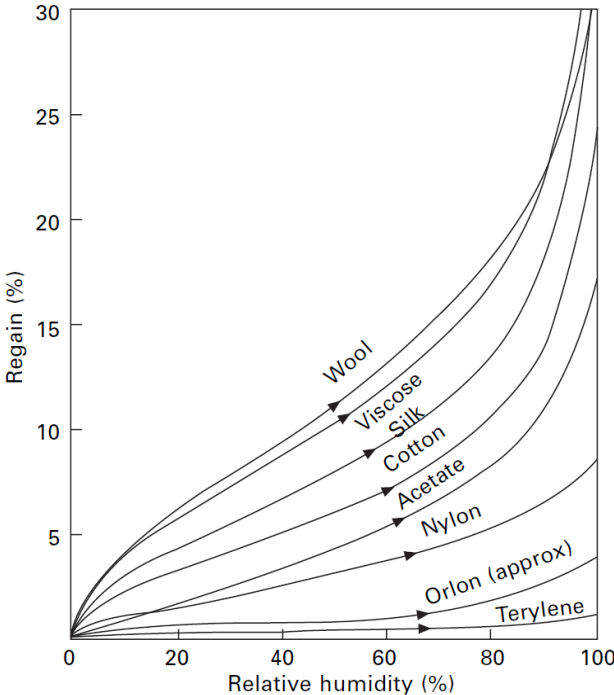

Figure 2.4 - Moisture content at different relative humidity values for some fibres

All these properties depends from temperature and moisture content; some experimental relationships giving these properties as a function of temperature and moisture content can be found in literature.

2.3 - Yarns structure

Yarns are the basic components of a fabric structure and their structure is very important for the comfort properties of fabrics.
Yarn structure depends from two parameters, yarn count and twist factor, that can be very different depending on the fabric structure that would be realized.

2.3.1 - Yarn count

Yarn count is defined as its mass per unit length; the international unit for count, defined from ISO, is the tex (*Tt*) that can be expressed as the mass in grams of 1000m of yarn.
In the past some others yarn count system has been defined such as:
  ➢ Denier, that is defined as the mass in grams of 9000m of yarn; it is used usually for silk and synthetic fibres
  ➢ Metric number, that is defined as the length in meters of 1g of yarn; it is used usually for wool yarns.
  ➢ Cotton count, that is defined as the number of hanks of 840yd that weight 1lb; it is used for cotton yarns.

2.3.2 - Twist factor

Twisting is used to make yarns more resistant to traction forces; applying a rotation to a bundle of fibres they will assume a helical arrangement.
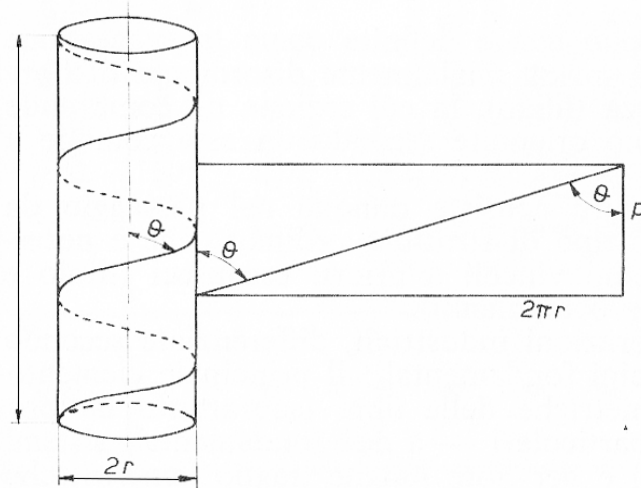A schematic representation is given in Fig. 2.5 [17].

Figure 2.5 - Helical arrangement representation

Twisting is defined as the number of coil per unit length and it is related to the pitch between the helixes using Eq. 2.1.

$$t = \frac{1}{p} \qquad [2.1]$$

where
p: helix pitch [m]
t: twist factor [turns/m]

2.3.3 - Yarn diameter

Yarn count and twist factor mainly influence the yarn diameter that is the first parameter that as to be known in order to be able to create a 3D model of any fabric.

Different expressions can be found in literature to calculate yarns diameter; one of the most used is reported in Eq. 2.2 [17].

$$d = 2 \cdot \sqrt{\frac{Tt}{\pi \cdot G \cdot 1000}} \qquad [2.2]$$

where
d: yarn mean diameter [mm]
Tt: yarn count [tex]
G: twist constant

Twist constant for some type of yarns can be defined from the twist factor (α) using the equations reported in Tab. 2.4 [17].

Yarn type	Twist constant [G]
Worsted yarns	*$0.58 + 0.25*10^{-4}*\alpha$*
Woollen yarns	*$0.47 + 0.28*10^{-4}*\alpha$*
Cotton yarns	*$0.55 + 0.28*10^{-4}*\alpha$*
Rayon yarns	*$0.60 + 0.27*10^{-4}*\alpha$*

Table 2.4 - Equation for twist constant calculation

Twist factor depends from the fibre material and from yarn application; some examples are reported in Tab. 2.5 [17].

Yarn	α
Cotton	
Knitwear	*77 - 92*
Weft	*92 - 108*
Warp	*124 - 139*
Strong warp	*170 - 201*
Crêpe	*216 - 278*
Worsted wool	
Knitwear	*54*
Soft	*63*
Medium	*73*
Strong	*82*
Extra strong	*92*

Table 2.5 - Twist factors

2.4 - Fabric structure

Fabrics can be divided into three main categories, namely woven, knitted and nonwoven fabrics; they differ for their construction methods and for their final application.
Woven fabrics are used mainly for suits, shirts, coats, etc... as they do not require highly elastic properties while knitted fabrics are used mainly for underwear, sweater, t-shirt and all types of garments that as to be able to shrink and to extend themselves.
Nonwoven fabrics are generally not used for clothing applications.

2.4.1 - Woven fabrics

A woven fabric is made binding orthogonally some vertical yarns, called warp yarns, with some horizontally yarns, called weft yarns.
A schematic representation is shown in Fig. 2.6.
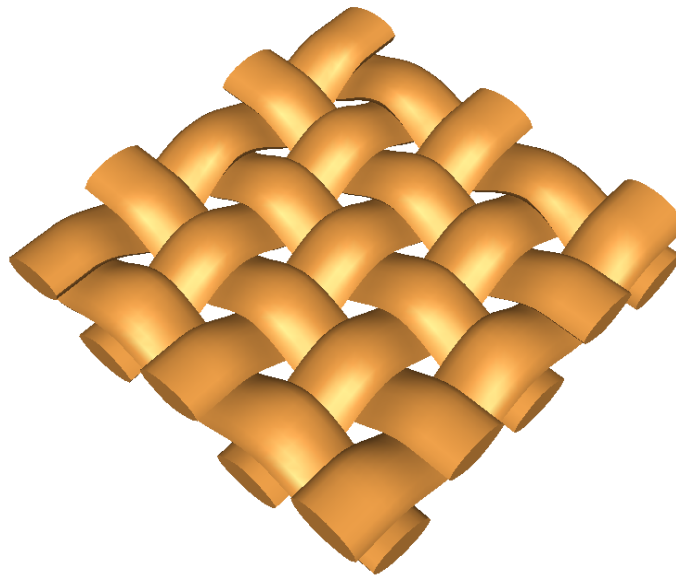
Figure 2.6 - Woven fabric

Woven fabrics can be divided into three main categories depending on the type of weave pattern:

> ➢ Plain
> ➢ Twill
> ➢ Satin

From these three fundamentals classes can be derived numerous other weave patterns, called derivative weaves.

As example, this three main categories are shown in Fig. 2.7.
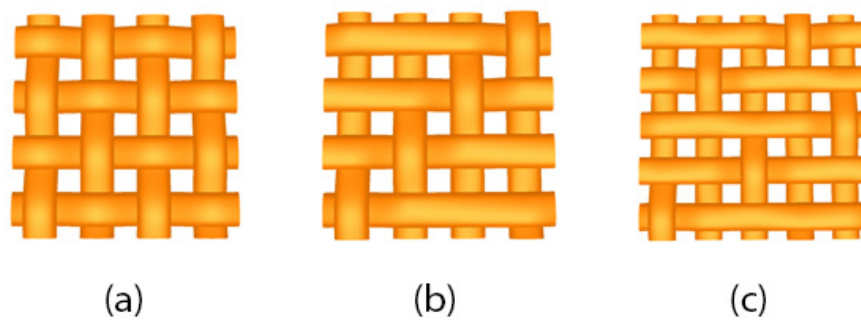

Figure 2.7 - Base weave pattern: (a) plain, (b) twill, (c) satin

Weave pattern are usually represented using a squared paper where every column represents one warp yarn while every row represents on weft yarn; when the warp yarn is above the weft yarn, the corresponding square is coloured in black while if the weft yarn is above the warp yarn the corresponding square is left uncoloured.
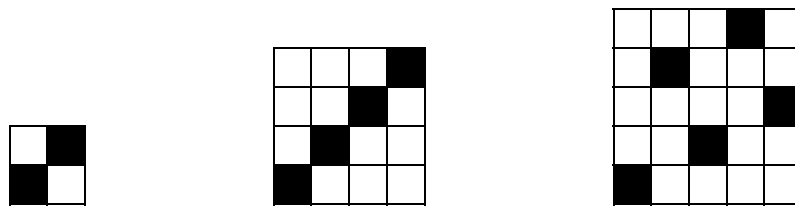

Figure 2.8 - Weave pattern schematic representation: (a) plain, (b) twill, (c) satin

Plain weave and their derivative patterns are the simplest pattern, characterized from a continuous movement of the warp yarns that moves above and under the weft yarns; a schematic representation is reported in Fig. 2.9.
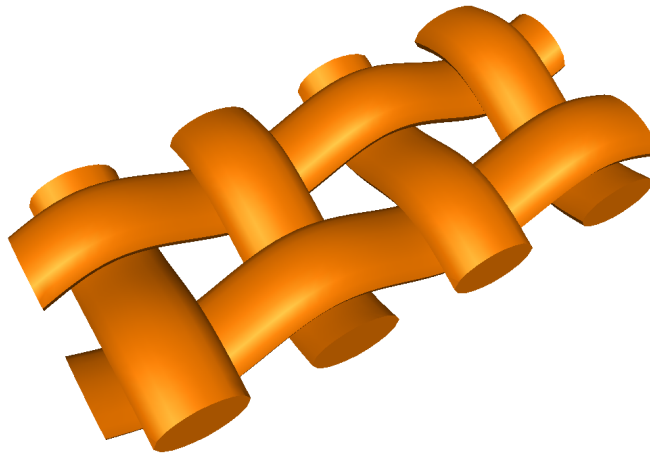
Figure 2.9 - Plain weave structure

Twill weave and their derivative patterns are characterized to have one front side, where warp yarns are more noticeable and one reverse side, where weft yarns are more evident. The minimum structure for twill pattern is composed of three warp and three weft yarns. As example in Fig. 2.10 are shown a 3-twill and a 5-twill fabric.
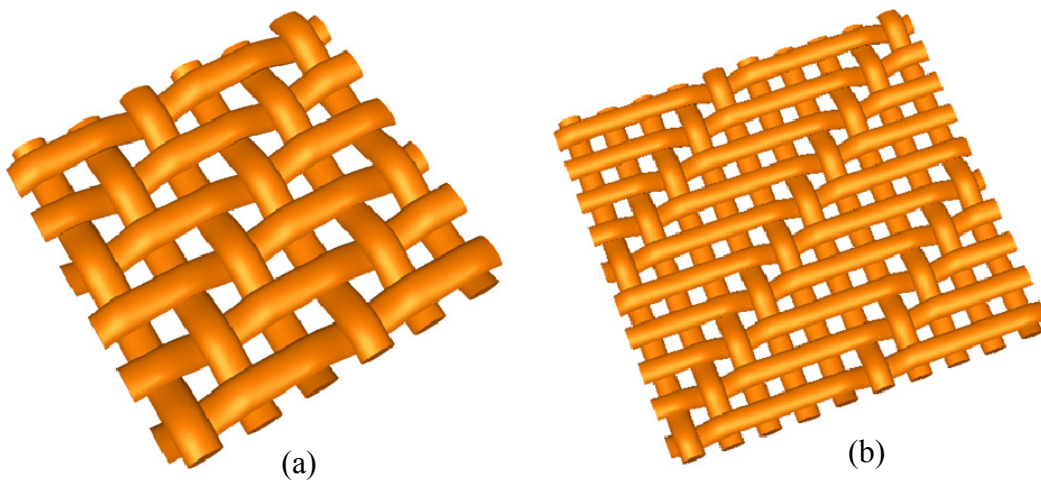

(a)

(b)

Figure 2.10 - Twill pattern: (a) 3x3, (b) 5x5

Satin weave and their derivative patterns are based on a non consecutive but regular distribution of the contact point between warp and weft yarns. The minimum ratio for satin pattern is five warp and five weft yarns. In Fig. 2.11 four different types of 7-satin fabrics are shown.
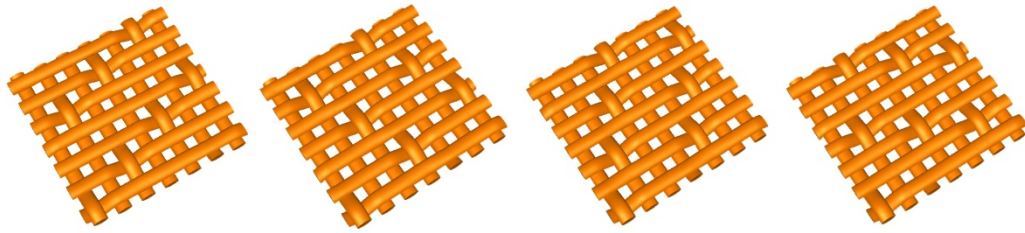
Figure 2.11 - Different types of satin fabrics

2.4.2 - *Knitted fabrics*

Knitted fabrics, unlike woven fabrics, are made using only one type of yarn, warp or weft yarn; it is formed by a sequence of a base element, called loop, both in the vertical and transversal way.

Loop is "a length of yarn that is forced to assume a curvilinear shape" [18] as shown in Fig. 2.13.

It can be divided into three part:

> ➢ Loop top (a)
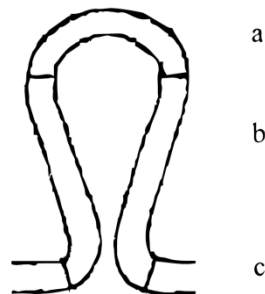> ➢ Loop side and bottom
> ➢ Half interloop

Figure 2.12 - Single loop

Knitted fabrics can be divided into two main categories, warp-knit and weft-knit fabrics. In weft-knit fabrics the interloop links two consecutive loops in horizontal direction while in warp-knit fabrics loops are knit vertically or diagonally.

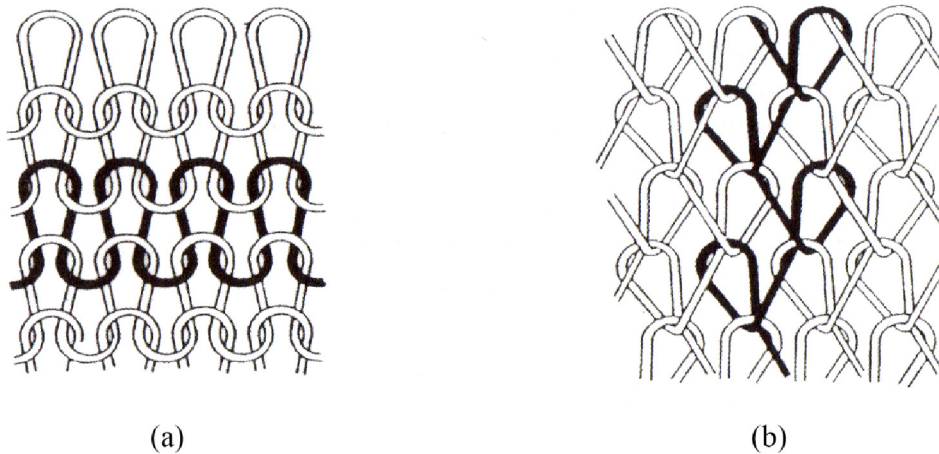As example a schematic representation is shown in Fig. 2.12 [18].

(a)   (b)

Figure 2.13 - Knitted fabrics: (a) weft knitted, (b) warp knitted

2.4.3 - Nonwoven fabrics

Nonwoven are defined as "a sheet or web of natural fibres and/or of chemically manufactured filaments, excluding paper, which have not been woven and can be bound together in different ways" [19].

Nonwoven is built without any weaving process and his raw material, loose fibres, are transformed into fabrics using chemical, mechanical or thermal processes that can be able to link together the fibres.

Nonwoven are today used in a wide range of sectors, thanks to their different technical characteristics and cheapness.

Table 2.6 [19] shows some application of nonwoven fabrics.

Personal care and hygiene	Clothing
- Baby diapers - Sanitary napkins - Products for adult incontinence - Dry and wet napkins - Cosmetic wipes - Breath-aiding nose strips - Adhesives for dental prosthesis - Disposable underwear	- Components for bags, shoes and belts - Insulating materials for protective wear - Outfits for fire protection - High visibility clothing - Safety helmets and industrial shoes - One-way work clothing - Clothing and shoe bag - Outfits for chemical and biological - protection

	• Interlinings
Medical use	**Leisure and travel**
• Caps, gowns, masks and overshoes for operating rooms • Curtains and blankets • Sponges, bandages and tampons • Bed linen • Pollution-controlled gowns • Gowns for medical examinations • Controlled-release plasters • Fastening tapes • Mattress fillings	• Sleeping bags • Suitcases, handbags and shopping bags • Containers for food transport • Vehicle headrests • CD slipcases • Pillowcases • Surfboards • Loudspeaker membranes
Household	**Upholstery**

• Handkerchiefs, wipers, towels
• Washing machine bags
• Vacuum cleaner bags
• Filters for kitchen hoods and air conditioners
• Coffee and tea bags
• Coffee filters
• Table linen
• Shoe and clothing bags
• Dust removing cloths and dusters
• Stain removers
• Descaling filters for boilers and kiers
• Food envelopes
	• Furniture
	  o Protections for shock absorbers
	  o Dustproof coverings
	  o Furniture reinforcements
	  o Armrest and backrest paddings
	• Beds
	  o Quilts and eiderdowns
	  o Dustproof coverings
	  o Spring protection
	  o Mattress components and linings
	• Curtains
	• Wallpapers
	• Carpet backing
	• Lampshades

School and office	**Filtering of liquids, air and gas**
• Book covers • Postal envelopes • Maps, signals and pennants • Blotting paper	• HEVAC/HEPA/ULPA filters • Filters for liquids: oil, beer, milk, • refrigerant liquids, fruit juices, etc. • Activated carbons • Odour control
Transports	**Industry**

• Boot linings • Shelves • Heat shields • Inner coatings of engine casing • Rugs, mats and sunshades • Oil filters • Waddings • Air filters in car cabin • Decoration fabrics • Airbags • Silencer materials • Insulating materials • Car roofs • Bands • Moquette backing • Seat covers • Car door borders	• Fabric coating • Electronics: floppy disks cases • Air filters, liquid and gas filters • Surface of clothing fabrics . veils • Insulating materials for cables • Insulating tapes • Abrasives • Conveyor belts • Reinforced plastics • PVC substrates • Fire barriers • Imitation leather • Sound absorbent panels • Air-conditioning • Battery separators for ion exchange and • catalytic separation • Anti-slip mats
Agriculture	**Geo-textiles**
• Covers for greenhouses and cultivations • Protections for seeds and roots • Fabrics for pests dominance • Pots for biodegradable plants • Materials for capillary irrigation	• Covers for road asphalting • Soil stabilization • Drainage • Sedimentation and erosion control • Water-hole sheathings • Sewers sheathings
Building industry	
• Insulation for roofs and tiles • Thermal and acoustic insulation • Boards for walls and false ceilings • Decorations for ceilings and walls	• Claddings for tubes • Casts for concrete • Stabilization of soils and foundations • Vertical drainage
Disposable cloths for industrial uses	

• Manufacturing, mechanical and maintenance industry
   o Machinery and equipment
	• Car industry
	   o Surface preparation before

cleaning
  o Sorbents for fluid and oil
  o Hand cleaning
	o Varnishing
	  o Polishing
	  o Sorbents for oil and chemical substances

• Transports
  o Vehicle cleaning and maintenance
  o Car window cleaning
	• Print works
	  o Machine cleaning and maintenance
	  o Sorbents for ink and other fluids
	  o Hand cleaning

• Food industry
  o Machine cleaning and maintenance
  o Hand cleaning
	• Cleaning industry
	  o Tools for delicate polishing
	  o Cleaning and maintenance equipment
	  o Dust removal

Table 2.6 - Non woven fabrics application

3 - Textile comfort properties evaluation

3.1 Introduction

In order to evaluate comfort properties of any textile fabric it is necessary to be able to measure some physical properties of the fabric itself.

Previous work such as that of Ress [21] shows that the factors that can affect the comfort performance are the heat transfer and the movement of moisture between the human body and the environment; in order to take into account these effects some physical test can be done in order to evaluate the following properties:

> ➢ Air permeability
> ➢ Thermal properties
> ➢ Liquid moisture transmission
> ➢ Moisture vapour transmission

These properties can be evaluated using different tests or, in case of full garments assemblies, using a thermal manikin in a climatic room [22]; using this method it is possible to determine the insulation of every garment area from the input of heat that is necessary to maintain a constant temperature. A more complex system is the sweating manikin that is provided with a sweating mechanism in order to take into account also the evaporative losses [23].

3.2 - Air permeability

Air permeability is perhaps the most important properties of a textile fabrics because it can affect the comfort properties in some different ways.

First of all if a fabric is permeable to air is generally also permeable to water both in liquid and in vapour state; this mean that liquid and vapour transmission properties are closely related to the air permeability value.

Secondly air permeability strongly affect also the thermal behaviour because thermal resistance of a fabric depends from the air trapped into the fabric itself; open fabrics generally present low thermal resistance values and can lead to a very uncomfortable feeling and in some extreme cases affect survival chances.

3.2.1 - Relationship between air permeability and fabric parameters

Many researchers have studied the air permeability properties in order to describe them in a theoretical way; the possibility to correlate air permeability with the structural parameters of yarns and fabrics is very important to be able to predict fabrics properties. Some work, such as that of Kondratskii [24], has been done considering that the air flow occurs only in the pores of the fabric structure and not through the yarns; this can be done using monofilament yarns or yarns with high twist factor. Assuming a small differential pressure and any jet compression Kondratskii proved that air permeability value depends only from the Reynolds number.

Alibert [25] derived a correlation between the cover factor of a fabric and its air permeability value while Köhler and Pietsch [26] shows that air permeability can be predicted from the structural parameters of fabrics.

Relation between the air permeability value and the specific fabric weight was derived from Kothari and Newton [27] and it is reported in Fig. 3.1.
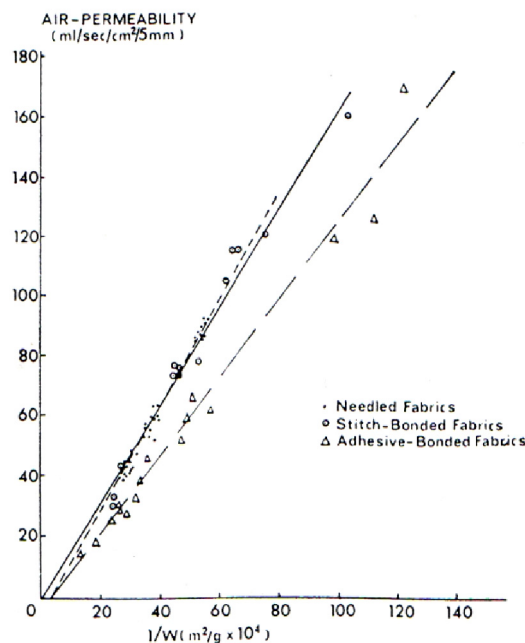

Figure 3.1 - Relation between air permeability and reciprocal of fabric weight per unit area (W)

for needle-punched, stitch-bonded and adhesive-bonded fabrics

Some recent works investigates the relationship between the fabric weave pattern and the resulting air permeability value such as that of Havlovà [28] and Fatahi [29] or Ogulata [30] for knitted fabric.

Not only the fabric structure but also the porosity and therefore permeability has been investigated from many researchers and some different models has been proposed [31]; recent works focus their attention also on the modelling of the real yarn structure, that is composed from numerous fibres, and then in the prediction of the permeability value [32].

3.2.2 - Air permeability test

As reported in UNI EN ISO 9237, air permeability is defined as the air flow velocity that cross perpendicularly a sample fabric once it is defined the test area, the pressure drop and the duration of the test.

A schematic scheme of an air permeability tester is shown in Fig. 3.2.
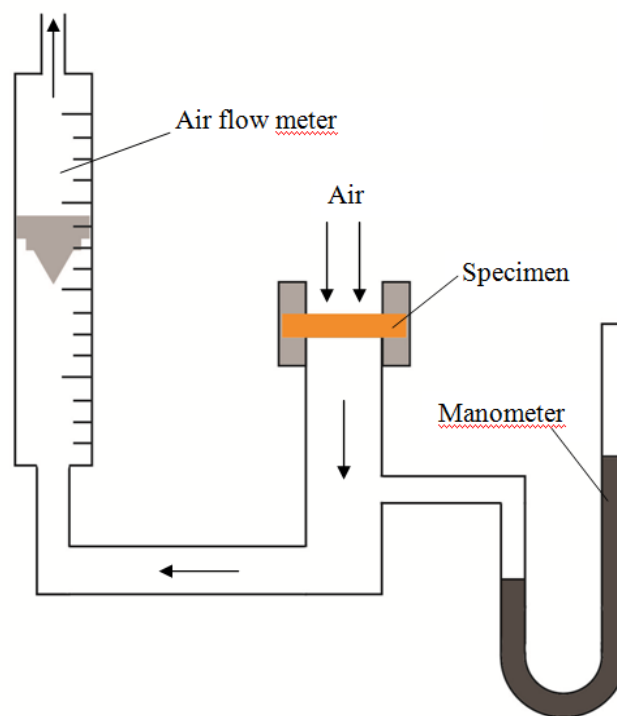

Figure 3.2 - Air permeability tester scheme

The test area can be of 5 cm^2, 20 cm^2, 50 cm^2 or 100 cm^2, the manometer should be able to measure a pressure drop of 50 Pa, 100 Pa, 200 Pa or 500 Pa and the flow meter should have an accuracy in the range of ±2%.

Every fabric has to be measured 10 times in different positions.

Air permeability (*R*) is usually expressed in mm/s and can be calculated from Eq. 3.1 [33].

$$R = \frac{\overline{q_v}}{A} * 167 \qquad [3.1]$$

where
$\overline{q_v}$: mean air flow rate [l/min]
A: test area [cm^2]
167: conversion factor from l/(min*cm^2) to mm/s

3.3 - Thermal properties

One of the most important properties of any garments is to protect the human body from extreme environmental condition, cold or hot cases, and to allow the heat exchange between the body and the environment in order to maintain a comfortable temperature.
The role of garments has been investigated by many authors. Clark [34] investigated the influence of garments using infra-red thermography and he proved that the presence of clothing interferes with the air layer near the skin surface that in case of a nude body moves around the body due to convection forces.
Hackenberg [35] affirmed that air temperature is the most important factor that affect skin temperature and so at low temperature clothing is very important to maintain body temperature, reducing the heat losses; on the other hand it is necessary that garments allow heat and moisture transfer if it is necessary.

3.3.1 - Relationship between thermal properties and fabric parameters

Thermal properties and so heat transfer through fabrics are affected from four main parameters, namely fabric thickness, enclosed still air, external air movement and moisture content.
These three parameters are the base of the work made by Yankelevich [36]; in his works he uses these three parameters to distinguish air permeable fabrics from hermetic ones. He shows that an increase in air permeability value leads to a reduction in thermal resistance, but only when a specific threshold value, that he called limit of hermetic state, is exceeded.
Other study made by Tilajka [37] shows that the heat insulation depends mainly by the fabric thickness while material and structure has no relevant effect; Weiner [38] focused his studies on the effect of thickness and weight and he shows that for a fixed weight the thermal insulation increases with thickness.
Some researchers focused their attention on the air trapped into the fabric.

Karlina [39] divided the air enclosed within a textile assembly into two different parts, a microlayer which is those between contacting surface of the materials and a macrolayer which is those between non-contacting surfaces; he shows that increasing both the micro and the macro layers the thermal insulation increases.

Fonseca [40] instead suggest that only the outer layer of a textile assembly is important for the thermal properties while the inner layers are necessary only to prevent the collapse of the outer layer onto the body and consequently the reduction of the quantity of air trapped into the assembly.

Another parameters that affects thermal properties is the moisture content.

Smirnov [41] in his studies analyze different samples of wool, wool-rayon and polyamide fabrics over a range of moisture content; he found that in the dry state the thermal conductivity of the different samples is almost the same, but increasing the moisture content, up to the bound water condition, the thermal conductivity of polyamide fabrics were lower than the wool ones. At higher water content the thermal conductivity of the different samples become again almost the same.

3.3.2 - Thermal resistance test

Thermal resistance is usually measured according to UNI EN ISO 5085-1 [42].

All the instrument are essentially based on three different methods:

> Single-plate method, which is used usually for outwear clothing where the outer surface of fabric is in contact with the ambient air
> Two-plate method, which is used for fabrics not directly in contact with the ambient air; the temperature gradient is measured using thermocouples.
> Guarded hot-plate method, which is suitable for thicker fabrics; a schematic representation is shown in Fig. 3.3 [43]
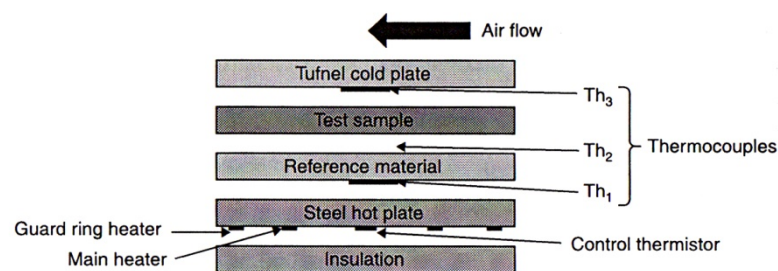

Figure 3.3 - Guarded hot-plate

Using a guarded hot plate for the test, heat resistance of the fabric can be calculated from Eq. 3.2 [43]:

$$R_{ct} = \frac{\bar{t}_{plate} - \bar{t}_a}{H_{dry}} - R_0 \qquad [3.2]$$

41

where

R_{ct}: heat resistance of the sample [m^{2}K/W]

t_{plate}: mean hot plate surface temperature [°C]

t_a: ambient temperature [°C]

H_{dry}: dry plate heat loss at ta (Hdry=0 if ta=tplate) [W/m^2]

R_0: heat resistance measured without sample [m^{2}K/W]

A common instrument that can be used in order to evaluate thermal properties of a fabric has been developed in 1987 at the Technical University in Liberec by L. Hes and it is called ALAMBETA; it is shown in Fig. 3.4 [44].
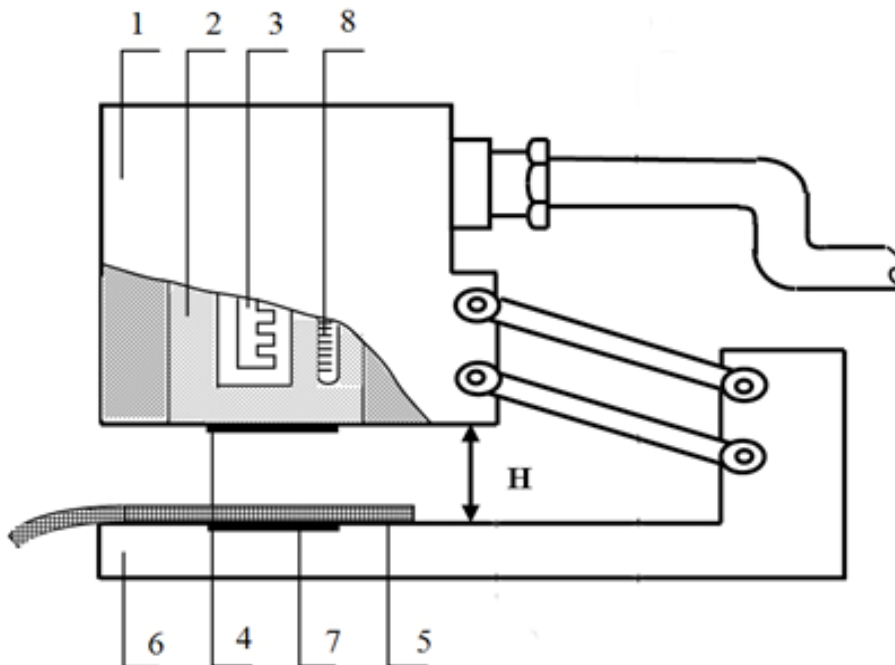

Figure 3.4 - ALAMBETA instrument

where

1) Measuring head
2) Metal block
3) Heating element
4) Heat flow sensor
5) Sample
6) Instrument base
7) Heat flow sensor
8) Thermometer

This instrument is able to measure thermal conductivity (λ), thermal resistance (R), the maximum level of the contact heat flow q_{max} and the sample thickness.

ALAMBETA is based on the definition of warm-cool feeling that is the feeling that a person gets when the human skin touches for a short period the textile fabric; the first instrument that was able to measure that characteristic, in terms of maximum level of the contact heat flow (q_{max}) was developed by Yoneda in 1983 [45].

Hes instead of q_{max} defines a thermal absorptivity (*b*) that can be calculated from Eq. 3.3:

$$b = \left(\lambda \rho c\right)^{1/2} \quad [3.3]$$

where
λ: thermal conductivity [W/(m*K)]
ρc: thermal capacity [J/(m^3*K)]

Referring to Fig.3.3, this instrument is based on a heat flow sensors (4) directly attached to a metal block (2) that is maintained at a constant temperature which is different from the sample temperature. Starting the measure the measuring head (1) drops down and touches the sample (5); when the hot head touch the sample its temperature rapidly change and the instrument measures the heat flow. Using a second heat flow sensor (7) it is also possible to determine heat that is exchanged with the surrounding air.

Usually in order to simulate a real condition the measuring head is heated up to 32°C, which is the mean human skin temperature while the sample is maintained at the room temperature (around 22°C).

3.4 - Liquid moisture transmission

Liquid moisture transmission through a fabric is the third fundamental properties that should be taken into account and it can be divided into two different aspects, namely water that comes from the environment and that should not reach the body surface and water produced as perspiration and that should be quickly removed from the body surface and transported to the outer clothing surface.

An ideal fabric should have pores big enough to allow water vapour transmission but the combination of pores size and fabric material, by surface tension, should not permit free access of water.

Water resistance treatments can be divided into two main categories:
   ➤ Waterproofing treatments
   ➤ Water-repellent treatments

Zysman [46] analyzes this two type of treatment and shows that a completely waterproof fabric is always impermeable both to air and water vapour.

Water-repellent behaviour is achieved using different fabrics treatment; the most common compound classes used to increase water-repellent properties are:

- ➢ Hydrocarbon hydrophobic (such as paraffin waxes, etc...)
- ➢ Silicon water repellents
- ➢ Fluorochemical repellents

Water is not only transported through the fabric but it is also absorbed; this mechanism depends mainly from the fibre material.
Generally there are three methods that can be used in order to increase liquid absorption:

- ➢ Physical modification of the structure
- ➢ Chemical treatment
- ➢ Coating techniques

Physical modifications can be achieved by creating micropores, incorporating different fibre types in the yarn or fabric structure and using particular fabric structures. The first case can be done during the extrusion process, varying the solvent removal velocity; in the second case natural or regenerated cellulosic fibres, that are highly hydrophilic, can be incorporated in the yarn or fabric structure. In the third case it is possible to create a double-layer fabric structure with an open structure fabric, with highly absorbency, at the inner surface and a close woven fabric, in order to not decrease the water resistance, at the outer surface.

The fundamental point is that liquid has to be transported at the outer fabric surface as quickly as possible and then evaporates in the environment.
The presence of liquid inside the fabric spoil the comfort properties in two different ways:

- ➢ The human skin perceives a sensation of wetness
- ➢ Liquid fill the free volume by throwing out the air and so the global thermal insulation of the fabric is reduced

3.4.1 - Liquid moisture properties test

Liquid moisture properties can be tested using the AATCC 195-2009 method; this test is able to analyze the liquid management in a fabric dynamically.
The most common instrument is the MMT (Moisture Management Tester) developed by SDL-Atlas; it can measure, for both woven and knitted fabrics, dynamic liquid transport properties in three different dimensions:

- ➢ Liquid transport on the inner surface (top) in the radial direction

➢ Liquid transport on the outer surface (bottom) in the radial direction
➢ Liquid transport from the inner to the outer surface
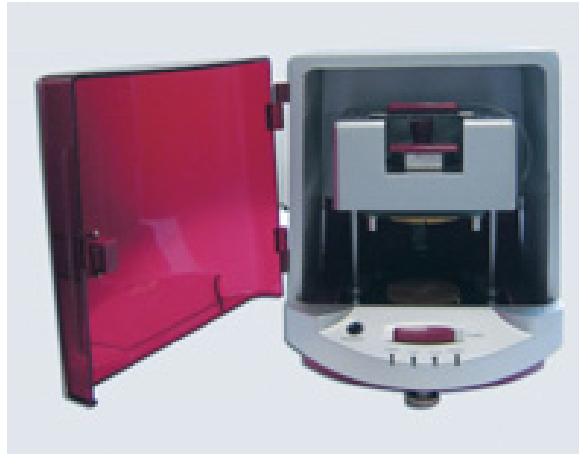
The MMT instrument is shown in Fig. 3.5.

Figure 3.5 - Moisture Management Tester

In order to estimate this three different processes it defines some different indexes:
➢ *Absorption rate (AR)*, that is the mean liquid absorption velocity at the inner and at the outer surface during the initial step
➢ *Wetting time (WT)*, that is the time required from the inner and from the outer surface to be wet; a wetting time of 120s, that is the test duration, means that the sample remains dry
➢ *Spreading speed (SS)*, that is the transport velocity from the initial contact point to the maximum wetting radius, calculated in the radial direction
➢ *Accumulative one-way transport capability (R)*, that represents the liquid transport from the inner to the outer surface, calculated as difference between the two wetting surfaces and over the time.
➢ *Overall liquid moisture management capability (OMMC)*, that is an index of the overall liquid transport capability calculated from the value of AR-bottom, SS-bottom and R.

The results provided by MMT depends from water resistance, water repellency and water adsorption characteristics of the sample, namely its geometrical structure, and from the wicking characteristics of its yarns and fibres.

3.5 - Moisture vapour transmission

Moisture vapour transmission is the fourth important properties for comfort evaluation; differing from the liquid transport in this case pores remain free and so the thermal insulation will not be affected.

Numerous studies have been made in order to analyze factors that can affect moisture transport properties.

Gogalla [47] in his work have studied the influence of the fabric properties and of the finishing treatments such as texturing, twist factor, mechanical treatments and chemical finishing.

Fabric structure influence has been investigated from several authors such as Weiner [48] that in his studies describes two mathematical models to predict the moisture vapour transmission; in the first study he analyze a fabric structure composed by pores filled with air and by a matrix structure made of a textile fibre in which moisture transmission can occur both in the pores volume and in the solid volume. In the second case he considers the fabric as an homogeneous porous media composed by a mixture of fibre and air; finally he shown that in order to predict moisture transport properties it were necessary to know only the density and the fabric thickness.

There are three ways to describe the moisture transport properties:
- ➤ Moisture vapour transmission rate (MVTR), which is the water vapour flow that passes through a unit area of fabric in a unit of time; the test is carried out under standard conditions of air temperature and humidity.
- ➤ Water vapour resistance, which is define as the equivalent thickness of still air which has the same resistance as the textile; for a clothing ensemble it is possible to add the resistance values of the different textile layers.
- ➤ Resistance to evaporative flow (R_{et}), which is the quantity which determines the latent or evaporative heat flux of a textile layer under steady state conditions effected by a partial water vapour pressure gradient perpendicular to the fabric [49].

The most common parameter used to describe the moisture transport is the water vapour resistance; there are two main instruments that can be used in order to obtain this parameters, the sweating guarded hot plate and the permetest.

Sweating guarded hot plate has been developed at the German Hohenstein Institute and it simulates the thermoregulation mechanism of the human skin; a schematic representation is given in Fig. 3.6 [43].
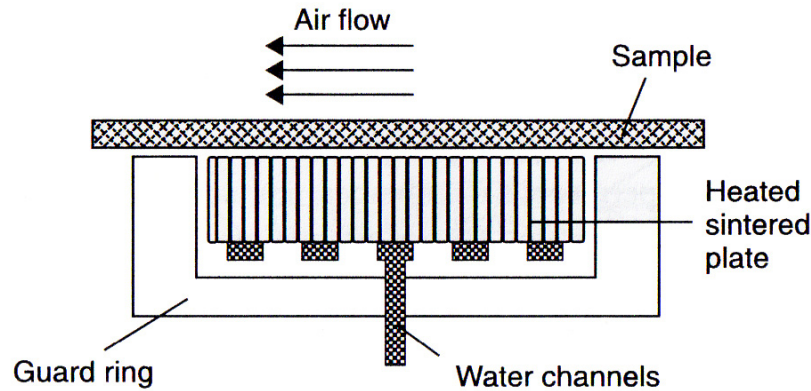
Figure 3.6 - Sweating guarded hot-plate

The instrument is composed from a porous stainless steel plate that, using electrical heater, is set to the temperature of the human skin (35°C); this plate is surrounded by a guard ring that is heated at the same temperature in order to avoid heat losses and so the heat flow can occurs only through the test sample.

Under the plate there are some channels in which water is supply; this water can evaporate through the pores of the plate and in this way it simulate the skin behaviour.

The instrument is usually used in a climatic room with user defined value of air temperature, humidity and velocity.

The vapour resistance can be calculated from Eq. 3.4:

$$R_{et} = \frac{p_{plate} - p_a}{H - H_{dry}} - R_{et()} \qquad [3.4]$$

where

R_{et}: vapour resistance of the sample [m²Pa/W]

p_{plate}: mean hot plate surface vapour pressure [Pa]

p_a: ambient vapour pressure [Pa]

H: total heat loss per square meter of wet plate area [W/m²]

$R_{et()}$: vapour resistance measured without sample [m²Pa/W]

H_{dry}: dry plate heat loss at ta (Hdry=0 if ta=tplate) [W/m²]

It is possible to define also the water vapour permeability index from Eq. 3.5 [43]:

$$I_{mt} = S\left(\frac{R_{ct}}{R_{et}}\right) \qquad [3.5]$$

where

I_{mt}: water vapour permeability index

R_{ct}: heat resistance of the sample [m²K/W]
R_{et}: vapour resistance of the sample [m²Pa/W]
$S = 60$ [Pa/K]

Water vapour permeability index is equal to zero for totally impermeable fabrics and it is equal to one for air.

Permetest has been developed by Hes [50] and it can measure both R_{ct} and R_{et} values. A schematic representation is given in Fig. 3.7 [43].
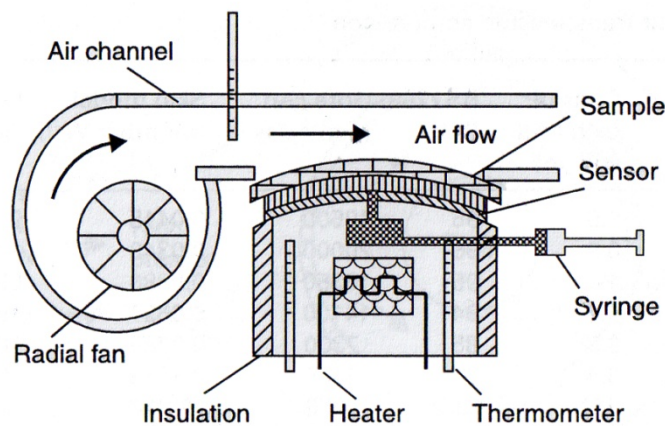

Figure 3.7 - Permetest

The instrument is composed from a curved porous surface with a diameter of 80mm place in an air channel, with air velocity that can be varied; the surface is moistened with water to simulate sweat evaporation and then it is covered by a semi-permeable membrane that allows only water in vapour phase to pass through it.
At the beginning the heat flow is measured without sample (q_0), then the sample is placed over the porous surface and, when the signal is steady, the heat flow (q_s) is recorded; these two values are both used to calculate the water vapour resistance (R_{et}) and the thermal resistance (R_{ct}) of the sample.

4 - Textile fabrics modelling

4.1 - Introduction

This work of thesis is based on the modelling of fabrics and on the prediction of their comfort properties in order to design new fabrics, in terms of material composition, structure, etc..., reducing the number of prototype samples and thus saving both time and money.

Fabrics modelling can be divided into two fundamental parts:

➢ 3D geometrical structure development
➢ Simulation of the comfort properties described in Chapter 3

The final goal of this project is to develop a prediction simulation method that can be used by textile designers and textile manufacturers.

4.2 - 3D geometrical modelling

The first to address is the modelling of the fabrics and yarns under a geometrical point of view.

As reported in Chapter 2, textile fabrics can be divided into three main categories, namely woven, knitted and non-woven, but for clothing application only woven and knitted fabrics are used.

In the geometrical modelling of fabrics three main aspects should be taken into account:

➢ Fibres distribution inside the yarn
➢ Yarn cross-sectional shape after the weaving process
➢ Warp and weft yarn path

4.2.1 - Fibres distribution inside the yarn

The first aspect that should be analyzed is how the fibres are combined in the yarn structure; yarn can be defined as a continuous structure composed by twisted fibres. Fibres, especially natural ones, are not all of the same dimension and consequently also the yarn diameter has a non uniform cross section; for modelling purposes it is useful to consider an ideal yarn with helical structure as shown in Fig. 4.1.
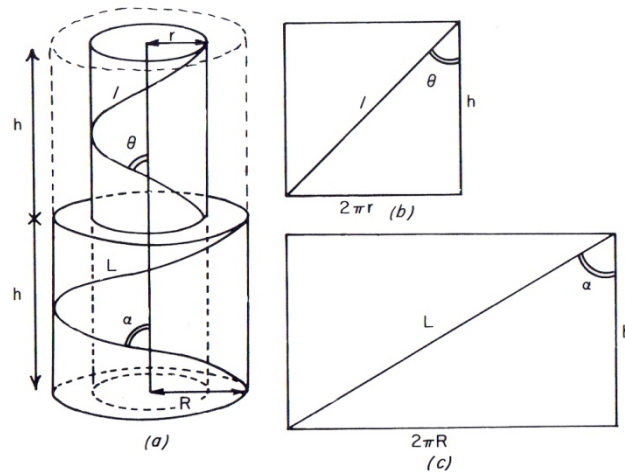

Figure 4.1 - Ideal yarn structure [51]

where
R: yarn radius
r: radius of the cylinder containing the helical path of a particular fibre
T: yarn twist
h: length of one turns of twist
α: surface angle of twist
θ: helical angle at radius *r*
l: length of fibre in one turn of twist, at radius *r*
L: length of fibre in one turn of twist, at radius *R*

Ideal yarn is assumed to have circular cross-sectional shape and to be composed of concentric cylinders of radius *r*; each fibre is assumed to follow an helical path around one of the cylinder of radius *r* so that the distance to the centre of the yarn remains constant. Going from the centre to the external radius the helix angle increase although the yarn twist remains constant.

Fig. 4.2 shows cross-sectional shapes of different yarns; it can be observed that, for almost all the yarns, the shape can be considered as circular.
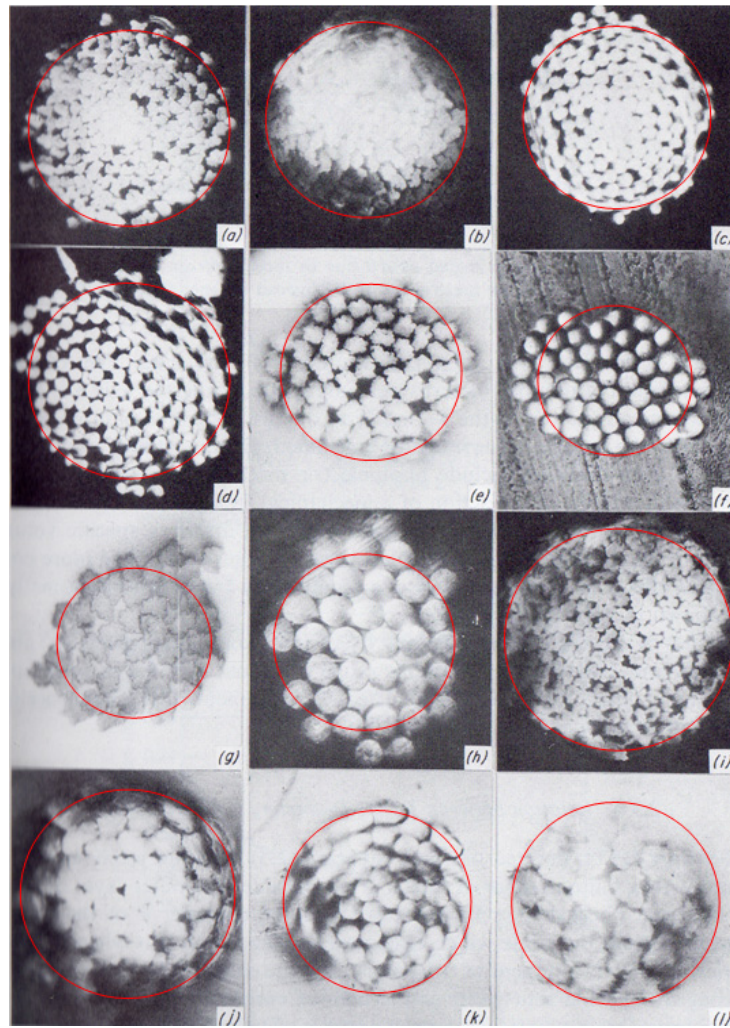
Figure 4.2 - Yarn cross sectional shape: (a,b,i) Tenasco, (c,d,h) Nylon,

(e,g,,j,l) Viscose, (f,k) Terylene [51]

For comfort properties simulation it is necessary to know some yarns parameters:
- ➢ Fibres material properties
- ➢ Yarn porosity
- ➢ Yarn permeability

The last two parameters should be derived from yarn structural parameters, namely yarn count and yarn twist that are independent variables.

Yarn porosity can be calculated as difference between the yarn cross section area and the area occupied by the fibres; in order to do this calculation the mean yarn diameter and the mean number of fibres should be calculated.

For mean yarn diameter calculation can be used Eq. 4.1 [17].

$$D = 2 \cdot \sqrt{\frac{Tt}{\pi \cdot G \cdot 1000}} \qquad [4.1]$$

where
D: yarn mean diameter [mm]
Tt: yarn count [tex]
G: twist constant (see Tab. 2.4)

The mean number of fibres in the yarn section can be estimated using Eq. 4.2 [17].

$$\overline{n}_s = \frac{Q \cdot Tt}{\frac{\pi}{4} \cdot \gamma \cdot d^2} \qquad [4.2]$$

where
$\overline{n_s}$: mean number of fibres in a cross-section
Tt: yarn count [tex]
γ: fibres density [g/cm^3]
d: fibres diameter [μm]
Q= 1000

The yarn porosity can be calculated using Eq. 4.3.

$$\varepsilon = 1 - \frac{A_f}{A_y} = 1 - \frac{\overline{n}_s \cdot d^2}{D^2} \qquad [4.3]$$

where
ε: yarn porosity
A_f: area occupied by the fibres
A_y: yarn cross section area
$\overline{n_s}$: mean number of fibres in a cross-section
d: fibres diameter [mm]
D: yarn mean diameter [mm]

Yarn permeability has been investigated by several authors in order to find a relationship between permeability and yarn porosity.
Gebart [52] in his studies derived a relationship between porosity and permeability for two different fibres packing arrays, quadratic and hexagonal, as shown in Fig. 4.3.
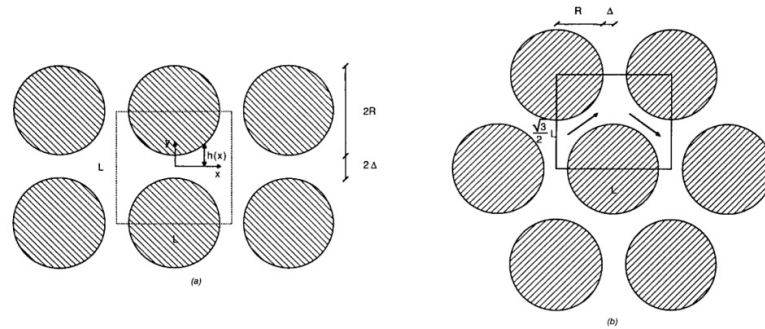
Figure 4.3 - Gebart fibres arrays

He proposed the relationship reported in Eq. 4.4.

$$\frac{K}{a^2} = C\left(\sqrt{\frac{1-\varepsilon_c}{1-\varepsilon}} - 1\right)^{5/2} \qquad [4.4]$$

where
K: permeability value
a: fibres radius
ε_c: critical value of porosity below which there is no permeating flow (fibres in touch)
ε: yarn porosity
C: geometric factor

ε_c and C can be calculated, for quadratic and hexagonal arrays, using the following equations.

Square array	$\varepsilon_c = 1 - \dfrac{\pi}{4} \qquad [4.5]$ $C = \dfrac{16}{9\pi\sqrt{2}} \qquad [4.6]$

Hexagonal array	$\varepsilon_c = 1 - \dfrac{\pi}{2\sqrt{3}}$ $\qquad$ $[4.7]$
	$C = \dfrac{16}{9\pi\sqrt{6}}$ $\qquad$ $[4.8]$

Table 4.1 - Φ_c and C parameters for square and hexagonal array

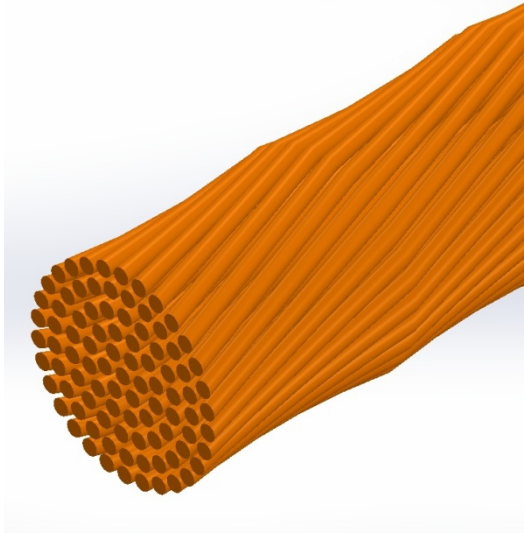An example of a 3D model of a yarn is shown in Fig. 4.4.

Figure 4.4 - Yarn 3D model, Count Nm 40, fibre diameter 18μm

4.2.2 - Yarn cross-sectional shape after the weaving process

During weaving process, yarns undergo some mechanical stress that cause deformation in the original cross-sectional shape of a yarn, as it can be seen in Fig. 4.5.

Figure 4.5 - Yarn deformation after weaving process [51]

The first researcher that investigated the geometrical modification due to the weaving processes was Pierce in 1937 [53]; his model is shown in Fig. 4.6.

He considered yarns as a highly incompressible medium, but at the same time highly elastic one, so that cross-sectional shape will remain circular; this model can be useful due to its simplicity but it is realistic only for very open structures where deformation of yarn section can be neglected.
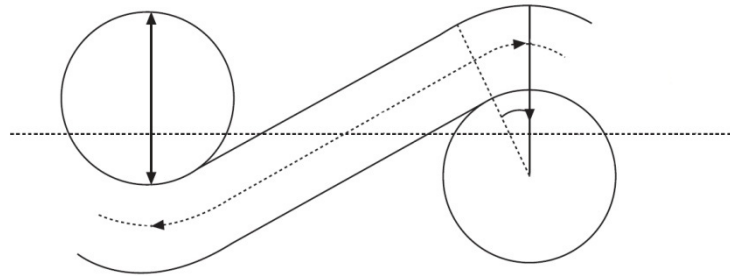

Figure 4.6 - Pierce model geometry [53]

For closed structures the flattening due to weaving process cannot be neglected.

Pierce in order to take into account this effect, proposed a modification of his model, introducing an elliptical shape, shown in Fig. 4.7.
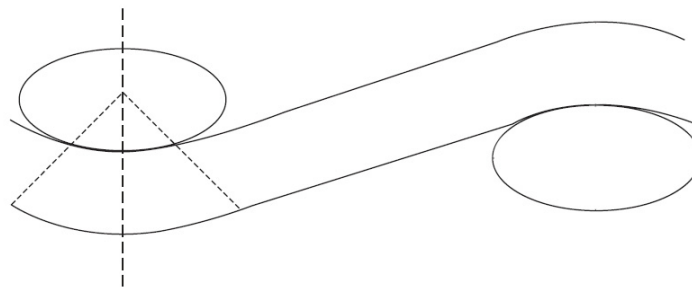

Figure 4.7 - Pierce elliptical geometry [53]

This model is suitable for medium open structures but it does not consider the jammed configuration; in order to overcome this problem a new cross-sectional model was proposed by Kemp in 1958 [54]; the geometrical representation is shown in Fig. 4.8. He proposed a cross-sectional shape based on a rectangular geometry closed at the ends by two semi-circular shape.
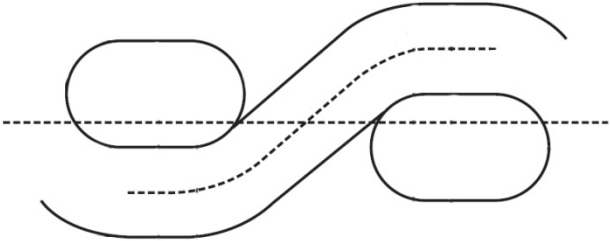
Figure 4.8 - Racetrack geometry proposed by Kemp [54]

In 1978 Hearle [55] proposed a more complex but more realistic model which considers a yarn deformation leading to a lenticular cross-sectional shape, as shown in Fig. 4.9.
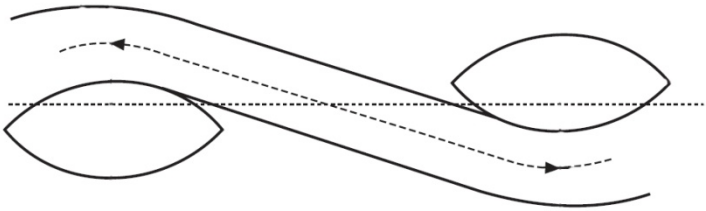

Figure 4.9 - Hearle lenticular geometry [55]

In Fig. 4.10 a comparison of the four different models with respect to a cross-section of a real fabric is shown.
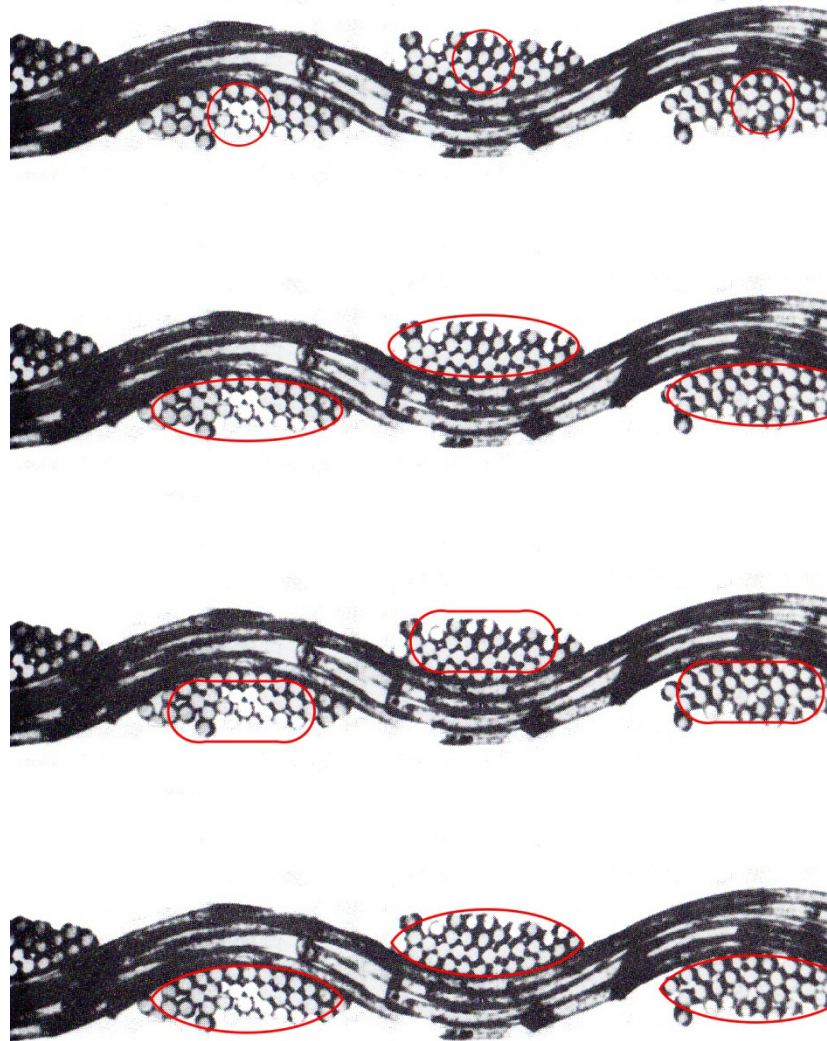
Figure 4.10 - Comparison between different models and a real fabric section [51]

4.2.3 - Yarn path of warp and weft

The third aspect to consider is the yarn path of both weft and warp yarns.
The yarn path has been described from the same researchers that has developed the cross-sectional models.

As reported in the previous section, Pierce model is the simplest way to describe both the yarn section and yarn path; he proposed a model that consist of eight equations and thirteen variables, that can be solved knowing five variables, usually the yarns spacing in the warp and weft, yarns diameters in the warp and weft and one crimp height.
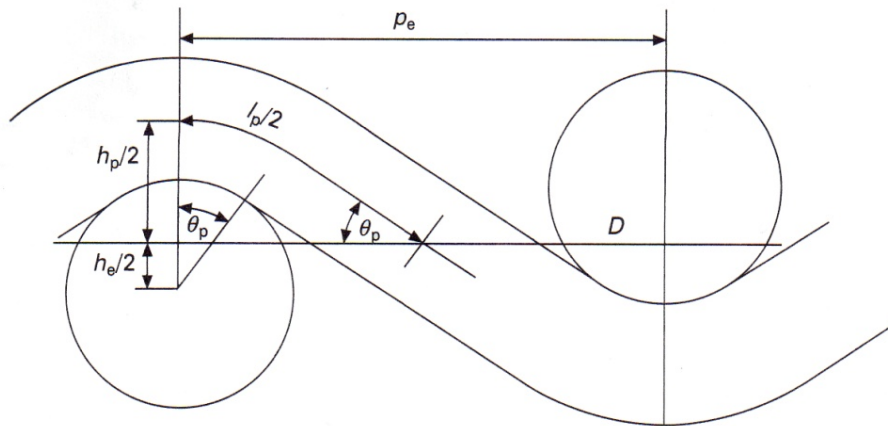
Figure 4.11 - Pierce model [53]

Pierce model can be described using the following equations:

$$p_p = \left(l_e - D\theta_e\right)\cos\left(\theta_e\right) + D\sin\left(\theta_e\right) \qquad [4.9]$$

$$p_e = \left(l_p - D\theta_p\right)\cos\left(\theta_p\right) + D\sin\left(\theta_p\right) \qquad [4.10]$$

$$h_p = \left(l_p - D\theta_p\right)\sin\left(\theta_p\right) + D\left(1 - \cos\left(\theta_p\right)\right) \qquad [4.11]$$

$$h_e = \left(l_e - D\theta_e\right)\sin\left(\theta_e\right) + D\left(1 - \cos\left(\theta_e\right)\right) \qquad [4.12]$$

$$D = d_e + d_p \qquad [4.13]$$

$$h_e + h_p = D \qquad [4.14]$$

$$c_e = \frac{l_e}{p_p} - 1 \qquad [4.15]$$

$$c_p = \frac{l_p}{p_e} - 1 \qquad [4.16]$$

where
h_p: modular height of the weft [mm]
h_e: modular height of the warp [mm]
c_p: crimp height of the weft [mm]

c_e: crimp height of the warp [mm]

D: sum of the warp and weft diameters [mm]

d_p: diameter of the weft [mm]

d_e: diameter of the warp [mm]

p_p: thread spacing between adjacent weft [mm]

p_e: thread spacing between adjacent warp [mm]

l_p: modular length of the weft [mm]

l_e: modular length of the warp [mm]

θ_p: weaving angle of the weft

θ_e: weaving angle of the warp

Kemp's racetrack model, shown in Fig. 4.12, can be considered as a derivation of the model proposed by Pierce in which only the yarn section has been changed from circular to racetrack one; the geometry between the line section S1 and line section S2 is equal to the geometry of the Pierce model.
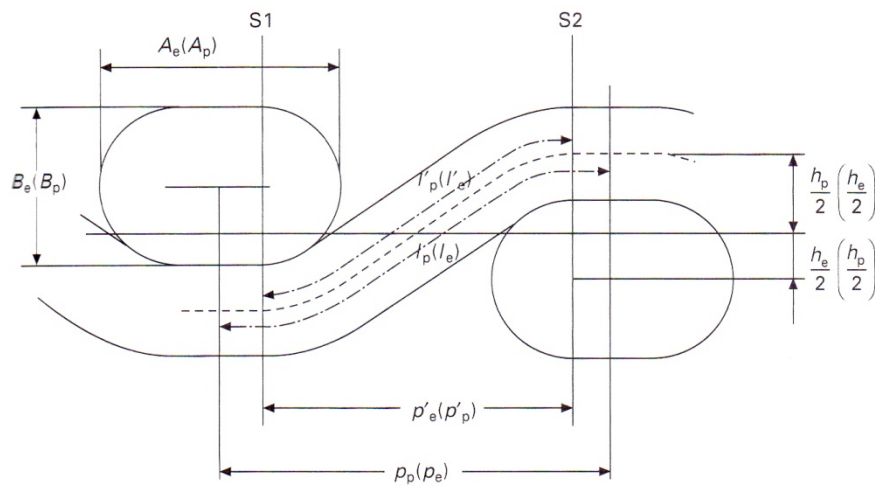

Figure 4.12 - Kemp model [54]

Ten variables, namely h_p, h_e, c_p, c_e, p_p, p_e, l_p, l_e, θ_p and θ_e, have the same definition as in the Pierce model while six new equations can be written as follow:

$$p'_p = p_p - \left(A_p - B_p \right) \qquad [4.17]$$

$$p'_e = p_e - \left(A_e - B_e \right) \qquad [4.18]$$

$$l'_p = l_p - \left(A_e - B_e \right) \qquad [4.19]$$

$$l'_e = l_e - \left(A_p - B_p \right) \qquad [4.20]$$

$$c'_e = \frac{l'_e - p'_p}{p'_p} = \frac{c_e p_p}{p_p - \left(A_p - B_p \right)} \qquad [4.21]$$

$$c'_p = \frac{l'_p - p'_e}{p'_e} = \frac{c_p p_e}{p_e - \left(A_e - B_e \right)} \qquad [4.22]$$

where
c'_p: crimp height of the weft between S1 and S2 [mm]
c'_e: crimp height of the warp S1 and S2 [mm]
p'_p: distance between S1 and S2 in weft direction [mm]
p'_e: distance between S1 and S2 in warp direction [mm]
l'_p: length of the path between S1 and S2 in weft direction [mm]
l'_e: length of the path between S1 and S2 in warp direction [mm]

Also the model proposed by Hearle can be considered as a derivation of the Pierce model in which the yarn section is formed joining two identical arcs.
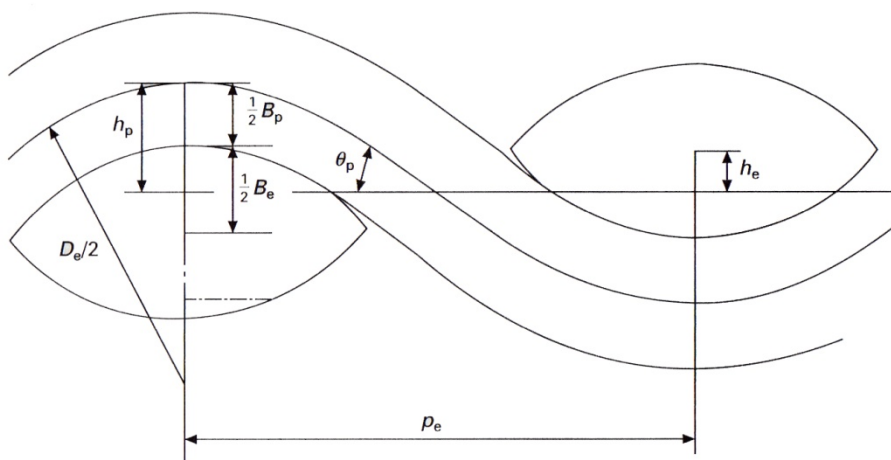A graphical representation is shown in Fig. 4.13.

Figure 4.13 - Hearle model [55]

Nine equations were derived to describe this model and every fabric geometry can be defined knowing seven parameters.

$$p_p = \left(l_e - D_e\theta_e\right)\cos\left(\theta_e\right) + D_e\sin\left(\theta_e\right) \qquad [4.23]$$

$$p_e = \left(l_p - D_p\theta_p\right)\cos\left(\theta_p\right) + D_p\sin\left(\theta_p\right) \qquad [4.24]$$

$$h_p = \left(l_p - D_p\theta_p\right)\sin\left(\theta_p\right) + D_p\left(1 - \cos\left(\theta_p\right)\right) \qquad [4.25]$$

$$h_e = \left(l_e - D_e\theta_e\right)\sin\left(\theta_e\right) + D_e\left(1 - \cos\left(\theta_e\right)\right) \qquad [4.26]$$

$$D_p = 2R_p + B_e \qquad [4.27]$$

$$D_e = 2R_e + B_p \qquad [4.28]$$

$$h_e + h_p = B_e + B_p \qquad [4.29]$$

$$c_e = \frac{l_e}{p_p} - 1 \qquad [4.30]$$

$$c_p = \frac{l_p}{p_e} - 1 \qquad [4.31]$$

Also in this model h_p, h_e, c_p, c_e, p_p, p_e, l_p, l_e, θ_p and θ_e have the same definition as in Pierce model and B_e and B_p are respectively the crimp heights of warp and weft yarns and R_e and R_p are the radii of the arcs used to represent the lenticular shape for both warp and weft yarns.

Using one of these models, and knowing some basic parameters of a fabric, is possible to describe the fabric under a geometrical point of view and therefore it is possible to reproduce this fabric in a 3D model, using any CAD software.

4.2.4 - TexGen

In order to predict comfort properties of a fabric, it is necessary to create a 3D model of its structure; in order to do this it is possible to use any CAD software but the most useful is TexGen.

TexGen is an open source software developed at the University of Nottingham in 1998 that is able to model the geometry of textile fabrics; in the last version it has a graphical interface and it is possible to create very simple structures using a wizard.
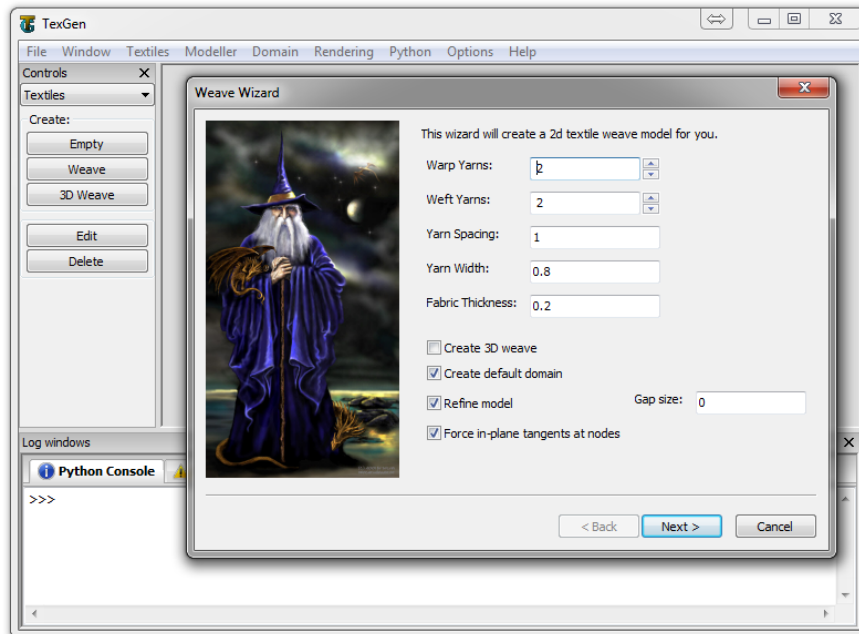

Figure 4.14 - TexGen wizard

Using this wizard it is only possible to create structures with the same threads spacing for both warp and weft; furthermore only elliptical shape is allowed and warp and weft yarns should have the same yarn count.

In order to create more complex structures it is possible to create separately both warp and weft yarns; in order to do this it is necessary to create one yarn and to set up both the nodes position in the space and the yarn section.
TexGen allows five different yarn section, as shown in Fig. 4.15, and it is also possible to rotate yarn around its main axis. The resulting yarn is shown in Fig. 4.16.
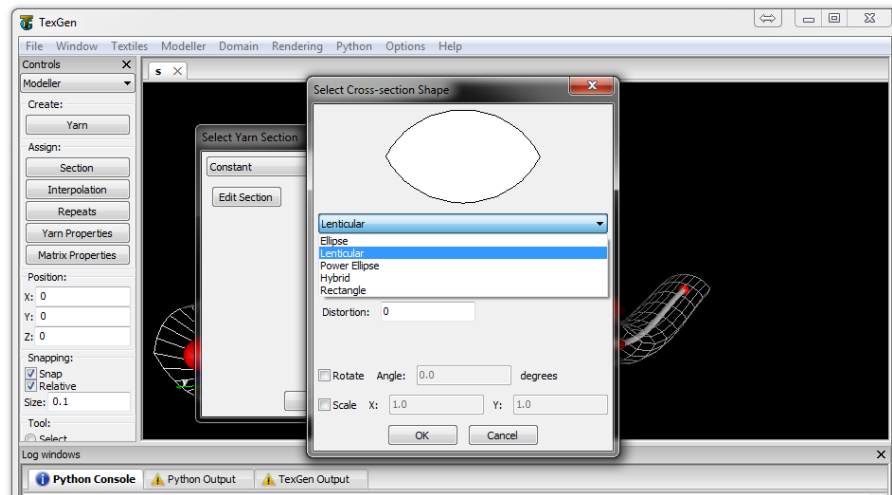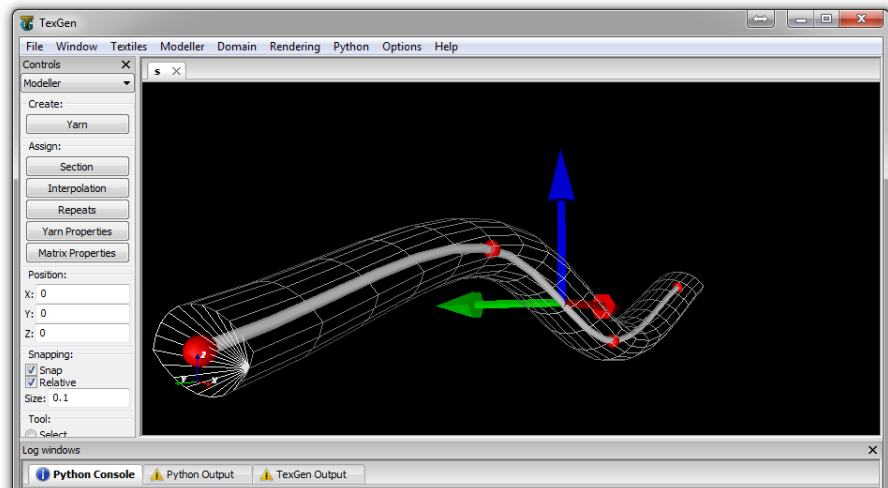
Figure 4.15 - TexGen yarns section

Figure 4.16 - TexGen yarn

In order to create 3D geometry every warp and weft yarn has to be defined; in this way it is possible to create any weave pattern. An example of the unit cell of a plain weave is shown in Fig. 4.17.
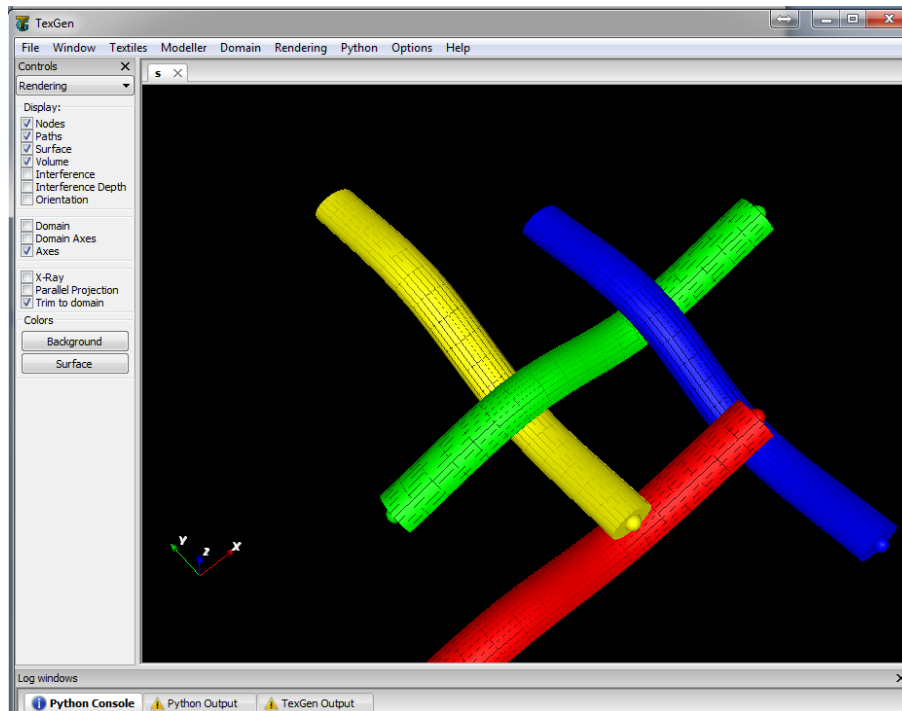
Figure 4.17 - Plain weave unit cell

TexGen is written in standard C++ and in order to create different textile structures it is possible to drive its Graphical Unit Interface using script written in Python.

This is the way used for this work of thesis because it is possible to define one script for every weave pattern (plain, twill, etc...) and then it is necessary to vary only the geometrical parameters in order to create a new textile fabric.

As example the script written for a plain weave with 21 ends/cm for warp yarns and 15 ends/cm for weft yarns is reported in Fig. 4.18.

```
                                                        PL22-15.py
# Create a textile
Textile = CTextile()


#Create weft yarn (trama)

# Create a lenticular section
Section = CSectionLenticular(0.398, 0.219)


# Create 4 yarns
Yarns = (CYarn(), CYarn())

# Add nodes to the yarns to describe their paths
Yarns[0].AddNode(CNode(XYZ(0, 0, 0)))
Yarns[0].AddNode(CNode(XYZ(0, 0.5, 0.218)))
Yarns[0].AddNode(CNode(XYZ(0, 1, 0)))


Yarns[1].AddNode(CNode(XYZ(0.714, 0, 0.218)))
Yarns[1].AddNode(CNode(XYZ(0.714, 0.5, 0)))
Yarns[1].AddNode(CNode(XYZ(0.714, 1, 0.218)))




# We want the same interpolation and section shape for all the yarns so loop over them all
for Yarn in Yarns:
    # Set the interpolation function
    Yarn.AssignInterpolation(CInterpolationCubic())
    # Assign a constant cross-section all along the yarn
    Yarn.AssignSection(CYarnSectionConstant(Section))
    # Set the resolution
    Yarn.SetResolution(30)
    # Add repeats to the yarn
    Yarn.AddRepeat(XYZ(1.428, 0, 0))
    Yarn.AddRepeat(XYZ(0, 1, 0))
    # Add the yarn to our textile
    Textile.AddYarn(Yarn)



#Create warp yarn

# Create a lenticular section
Section = CSectionLenticular(0.398, 0.219)


# Create 4 yarns
Yarns = (CYarn(), CYarn())

# Add nodes to the yarns to describe their paths
Yarns[0].AddNode(CNode(XYZ(0, 0, 0.218)))
Yarns[0].AddNode(CNode(XYZ(0.714, 0, 0)))
Yarns[0].AddNode(CNode(XYZ(1.428, 0, 0.218)))


Yarns[1].AddNode(CNode(XYZ(0, 0.5, 0)))
Yarns[1].AddNode(CNode(XYZ(0.714, 0.5, 0.218)))
Yarns[1].AddNode(CNode(XYZ(1.428, 0.5, 0)))




# We want the same interpolation and section shape for all the yarns so loop over them all
for Yarn in Yarns:
    # Set the interpolation function
    Yarn.AssignInterpolation(CInterpolationCubic())
    # Assign a constant cross-section all along the yarn
    Yarn.AssignSection(CYarnSectionConstant(Section))
    # Set the resolution
    Yarn.SetResolution(30)
    # Add repeats to the yarn
    Yarn.AddRepeat(XYZ(1.428, 0, 0))
    Yarn.AddRepeat(XYZ(0, 1, 0))
    # Add the yarn to our textile
    Textile.AddYarn(Yarn)



# Create a domain and assign it to the textile
Textile.AssignDomain(CDomainPlanes(XYZ(0, 0, -0.15), XYZ(1.428, 1, 0.35)));

# Add the textile with the name "cotton"
AddTextile("cotton", Textile)
```

Figure 4.18 - Plain weave 15/20 script

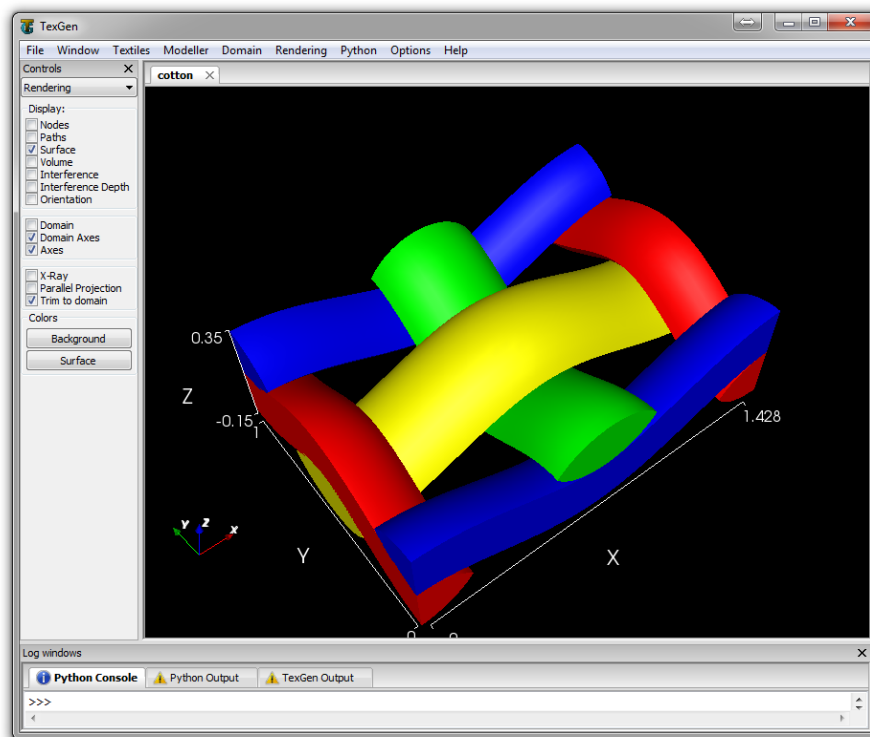The resulting geometry is reported in Fig. 4.19.

Figure 4.19 - Plain weave 3D model

Every textile structure analyzed in this work of thesis has been developed using the script method in order to obtain a realistic 3D structure of the different samples under investigation.

Once the structure has been created it is possible to export its 3D geometry in order to import it into the simulation software; geometries can be exported in IGES or STEP format.

4.3 - Air permeability

As reported in Chapter 3, air permeability is defined as the ability to allow air to flowing through a fabric.
In order to analyze the influence of different fabric structures, different 3D models, based on literature data, were realized and their air permeability value simulated using COMSOL Multiphysics®.

For this work, nine different fabric structures were analyzed, whose air permeability has been measured by Zupin et al. [56].

A schematic representation of the nine structures are shown in Fig. 4.20.

Plain weave
(PL)

Basket weave
(BW)

Filling rib
(R4/2)

Warp rib
(R2/4)

Twill 1/3
(T1/3)

Broken twill 1/3
(BT1/3)

Twill 2/2
(T2/2)

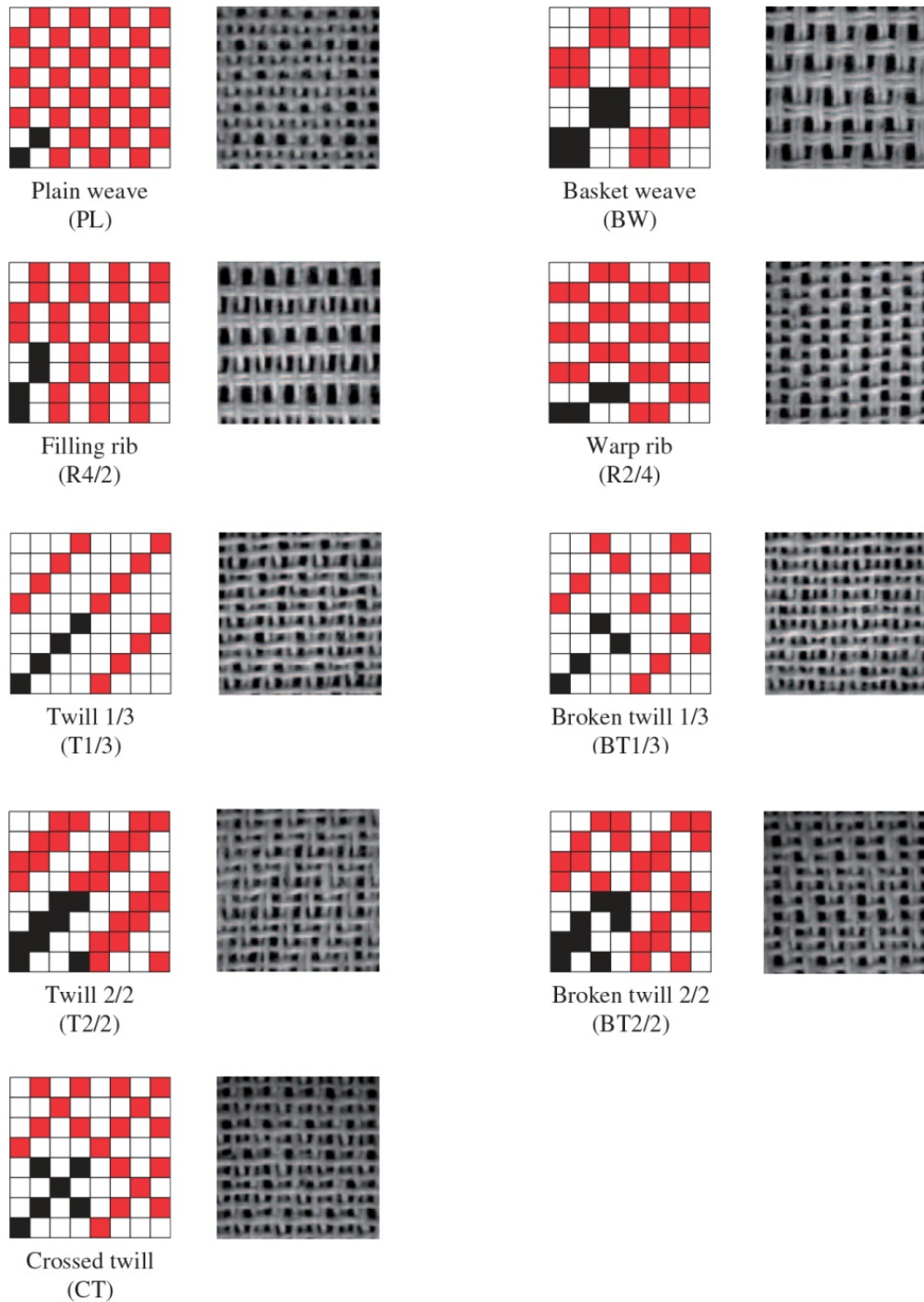Broken twill 2/2
(BT2/2)

Crossed twill
(CT)

Figure 4.20 - Fabric structures [56]

All fabrics were made of cotton and both warp and weft yarns had the same linear density (17x2 tex); one single yarn density, namely 22 ends/cm for warp and 15 picks/cm for weft yarns, was analyzed, except for the plain weave, for which also 22/20 density was simulated.

The fabrics characteristics are reported in Table 4.2.

Sample n°	Weave type	Set density Warp/Weft	Measured warp density	Measured weft density	Mass [g/m^2]	Thickness [mm]
1	Plain weave (PL)	22/15	21	15	143.91	0.439
2	Plain weave (PL)	22/20	21	20	166.59	0.438
3	Basket weave (BW)	22/15	21	15	140.52	0.506
4	Filling rib 4/2 (R4/2)	22/15	20	15	138.14	0.591
5	Warp rib 2/4 (R2/4)	22/15	22	14	143.77	0.549
6	Twill 1/3 (T1/3)	22/15	22	15	141.36	0.565
7	Broken twill 1/3 (BT1/3)	22/15	21.5	15	140.48	0.559
8	Twill 2/2 (T2/2)	22/15	21	15	141.78	0.508
9	Broken twill 2/2 (BT2/2)	22/15	21	15	139.01	0.522
10	Crossed twill (CT)	22/15	21	15	142.53	0.625

Table 4.2 - Fabrics characteristics (Zupin et al. [56])

Air permeability for each sample was carried out using the Air Permeability Tester III FX3300 LABOTESTER from Textest Instruments; the test pressure was set at 200 Pa and for each sample ten measurements were done.

4.3.1 - Simulation with COMSOL Multiphysics®

In order to simulate air permeability of the different 3D models created with TexGen, COMSOL Multiphysics® software was used.
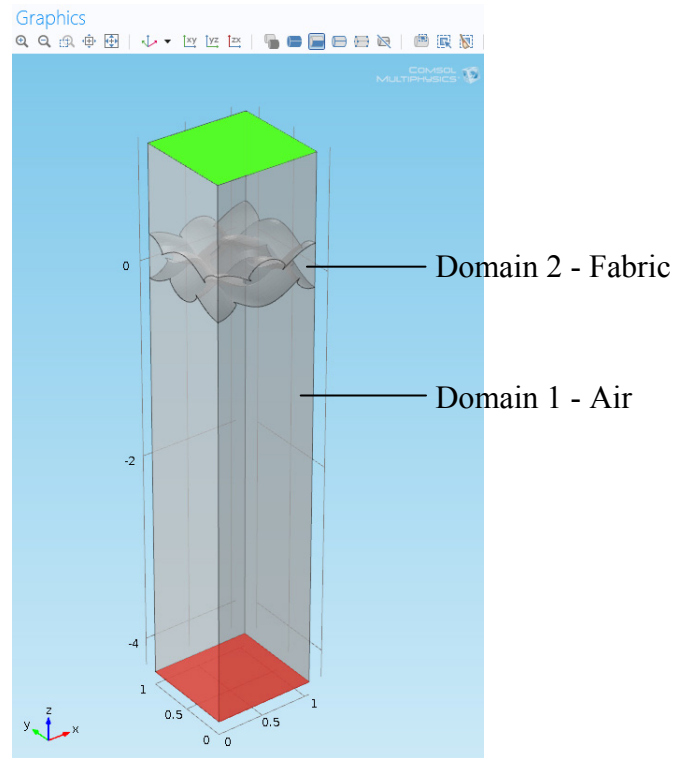A graphical representation of the geometry imported in COMSOL is given in Fig. 4.21.

Figure 4.21 - COMSOL geometry

The free and porous media flow interface was set in COMSOL; this allows to use Navier-Stokes equation for simulating the air free volume through yarns and the Brinkman equation for simulating the air flow inside yarns between the fibres (yarns were considered as a porous medium).

Four variables, namely three velocity components (u, v, w) and a pressure (p), are defined and the problem was solved as stationary (no time derivative terms); the temperature, depending on which the materials properties are calculated, was set at 20°C.

The textile fabric has been considered as infinite but, in order to reduce the computational time, a control volume that contains the base unit of every weave pattern has been modelled as shown in Fig. 4.21.

In the free volume one continuity equation and a equation for conservation of momentum are set:

$$\rho(u \cdot \nabla) = \nabla \cdot \left[-pI + \mu(\nabla u + (\nabla u)^T) - \frac{2}{3}\mu(\nabla \cdot u)I \right] + F \qquad [4.32]$$

$$\nabla \cdot (\rho u) = 0 \qquad [4.33]$$

where
ρ: density [kg/m^3]

u: velocity vector [m/s]
p: pressure [Pa]
μ: dynamic viscosity [Pa·s]
F: volume force vector [N/m^3]

In the porous domain, using the Free and Porous Media Interface, the Brinkman equation is used; this model extend the Darcy model in order to take into account the viscous transport in the momentum balance.

The continuity and momentum equations that has been set are:

$$\nabla \cdot (\rho u) = 0 \qquad\qquad [4.34]$$

$$\frac{\rho}{\varepsilon_p}\left((u \cdot \nabla)\frac{u}{\varepsilon_p}\right) = \nabla \cdot \left[-pI + \frac{\mu}{\varepsilon_p}(\nabla u + (\nabla u)^T) - \frac{2\mu}{3\varepsilon_p}(\nabla \cdot u)I\right] - \left(\mu k^{-1}\right)u + F \qquad [4.35]$$

where
ρ: density [kg/m^3]
u: velocity vector [m/s]
p: pressure [Pa]
μ: dynamic viscosity [Pa·s]
F: volume force vector [N/m^3]
ε_p: porosity
k: permeability tensor [m^2]

The porous media volume has been defined using the characteristics of the cotton yarns calculated using the relationship reported in Chap. 4.2.1 that are reported in Tab. 4.3.

Porosity	0.58
Hexagonal array permeability	$1.35*10^{-11}$ [m^2]
Square array permeability	$1.64*10^{-11}$ [m^2]

Table 4.3 - Porous matrix properties

Boundaries conditions have been defined for inlet, outlet and for the side walls of the control volume.

Constant pressure has been defined as inlet condition and it has been set at 200Pa (relative pressure) as in the tests carried out by Zupin [56]; this is achieved by setting up the following equations for pressure with no viscous stress condition:

$$p = p_0 \qquad\qquad [4.36]$$

$$\left[\mu(\nabla u + (\nabla u)^T) - \frac{2}{3}\mu(\nabla \cdot u)I \right] \cdot n = 0 \quad [4.37]$$

The outlet relative pressure was set at 0 Pa using the following equation:

$$\left[-pI + \mu(\nabla u + (\nabla u)^T) - \frac{2}{3}\mu(\nabla \cdot u)I \right] \cdot n = -p_0 \cdot n \quad [4.38]$$

At the side wall a symmetry boundary condition has been used in order to consider an infinite textile fabric; this condition consists into two equations that prescribe no penetration and the vanishing of the shear stresses.

$$u \cdot n = 0 \qquad\qquad [4.39]$$

$$\left[-pI + \mu(\nabla u + (\nabla u)^T) - \frac{2}{3}\mu(\nabla \cdot u)I \right] \cdot n = 0 \quad [4.40]$$

For all the simulations the mesh has been created using tetrahedral elements for both free and porous domain; the main characteristics of the mesh elements are reported in Tab. 4.4.

Maximum element size [mm]	0.15
Minimum element size [mm]	0.006
Maximum element growth rate	1.2
Number of elements	10^6 - $1.6 \cdot 10^6$

Table 4.4 - Mesh characteristics

The results of the simulations compared to the experimental values reported by Zupin [56] are shown in Tab. 4.5.

N°	Weave type	Measured [mm/s]	Coefficient of variation [%]	Calculated [mm/s]
1	Plain weave (PL)	2391.67	8.20	2316
2	Plain weave (PL)	1571.67	1.58	1526
3	Basket weave (BW)	3065	2.14	2989
4	Filling rib 4/2 (R4/2)	3491.67	1.61	3531
5	Warp rib 2/4 (R2/4)	3288.33	1.61	3207
6	Twill 1/3 (T1/3)	3505.83	2.94	3586
7	Broken twill 1/3 (BT1/3)	3501.67	2.00	3596
8	Twill 2/2 (T2/2)	3016.25	1.29	3051
9	Broken twill 2/2 (BT2/2)	3169.17	1.91	3099
10	Crossed twill (CT)	3465.83	1.82	3411

Table 4.5 - Air permeability values, measured and calculated

In order to compare data obtained from simulations and literature data, a parity plot is shown in Fig. 4.22.
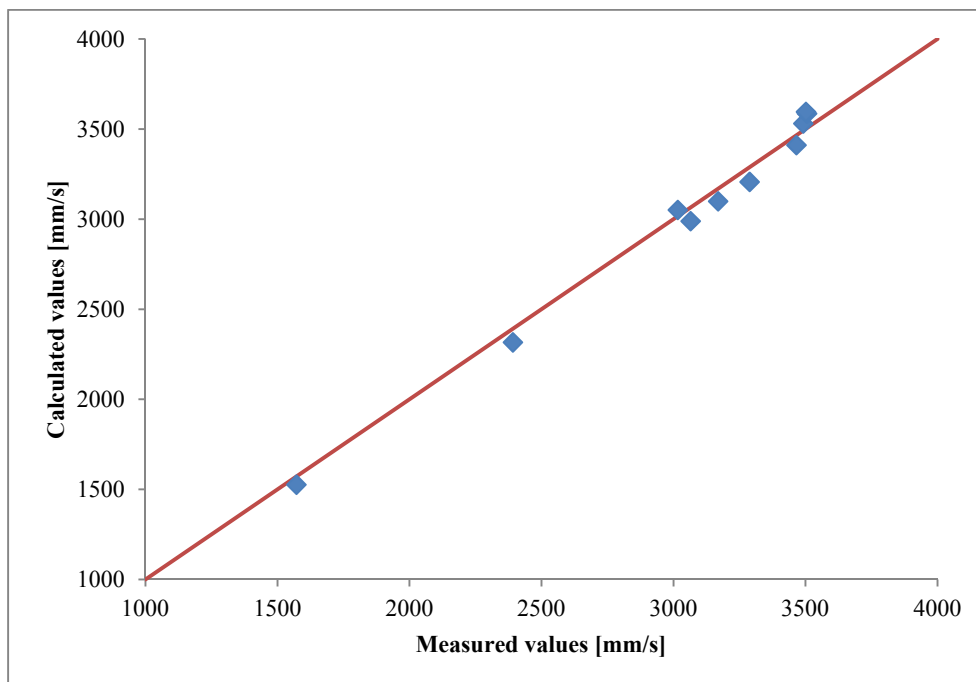
Figure 4.22 - Air permeability data, parity plot

As it can be observed, a good agreement between the literature data and the simulations results, with a maximum error of about 3% has been obtained.

These results confirms that air permeability of different woven fabrics can be predicted with good accuracy using only the basic design parameters of any fabric.

4.4 - Thermal resistance

The second property that has been analyzed is the thermal resistance.

As for air permeability, different fabrics structures has been created using TexGen and then their thermal resistance has been calculated using COMSOL Multiphysics®.

Fabrics are based on work done by Bhattacharjee [57] that has investigated plain, twill and satin weave pattern with different yarn count and warp and weft densities; all the fabrics are made of cotton so the thermal conductivity of the fibres can be set at 0.06 W/(m·K).

Properties of the different fabrics taken into account are reported in Tab. 4.6.

Sample n°	Weave type	Warp count [Ne]	Weft count [Ne]	Measured warp density	Measured weft density	Thickness [mm]
1	Plain weave (PL)	2/40	2/40	48	24	0.24
2	Plain weave (PL)	2/40	2/40	40.8	29.6	0.21
3	Twill 2/2 (T2/2)	2/40	2/38	48	22.4	0.46
4	Twill 2/2 (T2/2)	2/40	2/40	48.8	20.8	0.49
5	Twill 3/1 (T3/1)	20	16	49.6	25.6	0.24
6	Twill 3/1 (T3/1)	20	20	44	23.2	0.32
7	Twill 3/1 (T3/1)	2/38	2/54	51.2	36.8	0.38
8	Twill 3/1 (T3/1)	2/50	2/50	60	28	0.27
9	4 end satin (S4)	2/40	2/40	48.8	24.8	0.47
10	4 end satin (S4)	2/40	2/40	49.6	20	0.42

Table 4.6 - Fabrics properties

Thermal resistance for each sample was carried out using the ALAMBETA instrument and the test temperature was set at 32 °C [57].

4.4.1 - Simulation with COMSOL Multiphysics®

In order to analyze the thermal resistance of each sample, 3D geometries has been created, using TexGen, in the same way as for air permeability simulations; using these geometries the results obtained from COMSOL do not agree with the results reported in literature. This is caused by the test mode used from ALAMBETA instrument; in fact, fabric is placed between two measuring head that applies a pressure over the fabric. This leads to a reduction of the thickness that cannot be considered as the real thickness of the fabric and also to an increasing in the contact surface area between the fabric and the measuring head, as shown in Fig. 4.23.
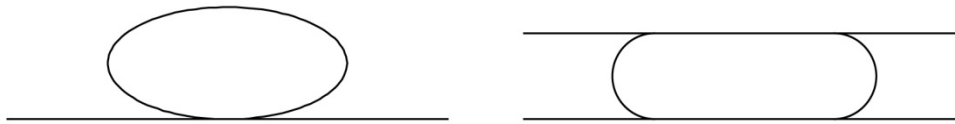
Figure 4.23 - Yarn crushing due to ALAMBETA test

For this reason, for thermal resistance simulations, the real 3D geometry cannot be used; to overcome this problem a simplified 3D geometry has been created.
Starting from the 3D geometries built using TexGen, some flat porous plates, with holes in the same position as in the 3D geometries, has been designed directly into COMSOL Cad Module; thickness of the simplified geometries has been set at 75% of the real thickness in order to take into account the flattening due to ALAMBETA instrument.

An example of these geometries, with the corresponding 3D real model, is shown in Fig. 4.24.
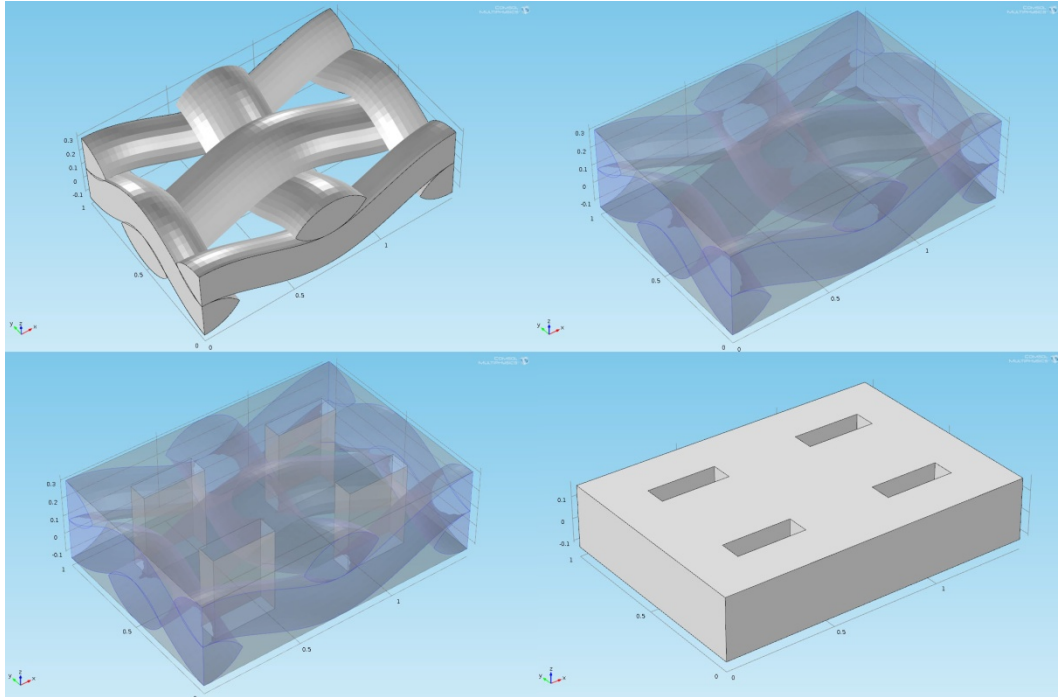
Figure 4.24 - Simplified fabric geometry based on 3D model

For thermal resistance simulations, heat transfer in porous media interface has been set in COMSOL; only one independent variable, namely temperature, has been taken into account.

Fluid has been considered immobile inside the macro and micro pores due to the presence, in ALAMBETA instrument, of two measuring head that are in contact with the fabric surface so that air is trapped between them.

The textile fabric has been considered as infinite but, in order to reduce the computational time, a control volume that contains the base unit of every weave pattern has been modelled as shown in Fig. 4.24.

All the simulations were run as stationary problems and so no time derivative terms appear in the governing equations.

In the porous domain the following equation of the heat transfer equation has been used:

$$\rho C_p u \cdot \nabla T = \nabla \cdot \left(k_{eq} \nabla T \right) + Q \qquad [4.41]$$

where
ρ: fluid density [kg/m^3]
C_p: fluid heat capacity [J/(kg·K)]
u: fluid velocity field [m/s]
k_{eq}: equivalent thermal conductivity [W/(m·K)]
Q: heat source [W/m^3]

T: temperature [K]

For all simulations the heat source is zero and the fluid velocity is zero in all the spatial directions.

The equivalent thermal conductivity has been defined as:

$$k_{eq} = \theta_p k_p + \theta_l k = \theta_p k_p + \left(1 - \theta_p\right) k \qquad [4.42]$$

where
k_{eq}: equivalent thermal conductivity [W/(m·K)]
θ_p: solid volume fraction
k_p: solid thermal conductivity [W/(m·K)]
θ_l: fluid volume fraction
k: fluid thermal conductivity [W/(m·K)]

In the fluid domain, inside the macro-pores, the heat equation can be written as:

$$\rho C_p u \cdot \nabla T = \nabla \cdot \left(k \nabla T\right) + Q \qquad [4.43]$$

where
ρ: fluid density [kg/m³]
C_p: fluid heat capacity [J/(kg·K)]
u: fluid velocity field [m/s]
k: fluid thermal conductivity [W/(m·K)]
Q: heat source [W/m³]
T: temperature [K]

The solid matrix of the porous volume has been defined using the characteristics of the cotton fibres that are reported in Tab. 4.7.

Thermal conductivity	0.06 [W/(m·K)]
Density	1540 [kg/m³]
Heat capacity at constant pressure	1340 [J/(kg·K)]

Table 4.7 - Cotton fibres characteristics

Boundaries conditions has been defined for the top, the bottom and for the side walls of the control volume.

At the bottom surface a constant temperature of 32°C has been set while for the top surface a temperature of 20°C has been considered; as for air permeability simulations for the side walls a symmetry condition has been used in order to consider an infinite fabric.

The symmetry condition can be written as:

$$-n \cdot (-k \cdot \nabla T) = 0 \qquad [4.44]$$

For all the simulations the mesh has been created using tetrahedral elements for both free and porous domain; the main characteristics of the mesh elements are reported in Tab. 4.8.

Maximum element size [mm]	0.02
Minimum element size [mm]	0.001
Maximum element growth rate	1.2
Number of elements	30000 - 50000

Table 4.8 - Mesh characteristics

As it can be seen, in case of thermal simulations mesh have less elements that for air permeability simulations; this is due to the simplest geometry that has been used.

The results of the simulations compared to the experimental values reported by Bhattacharjee [57] are shown in Tab. 4.9.

Sample n°	Weave type	Measured thermal resistance [(K·m²)/W]	Calculated thermal resistance [(K·m²)/W]
1	Plain weave (PL)	0.0079	0.0075
2	Plain weave (PL)	0.0091	0.0083
3	Twill 2/2 (T2/2)	0.0036	0.0037
4	Twill 2/2 (T2/2)	0.0047	0.0044
5	Twill 3/1 (T3/1)	0.0070	0.0073
6	Twill 3/1 (T3/1)	0.0039	0.0035
7	Twill 3/1 (T3/1)	0.0085	0.0089
8	Twill 3/1 (T3/1)	0.0070	0.0065
9	4 end satin (S4)	0.0031	0.0034
10	4 end satin (S4)	0.0031	0.0033

Table 4.9 - Thermal resistance values, measured and calculated

In order to compare data obtained from simulations and literature data, a parity plot is shown in Fig. 4.25.
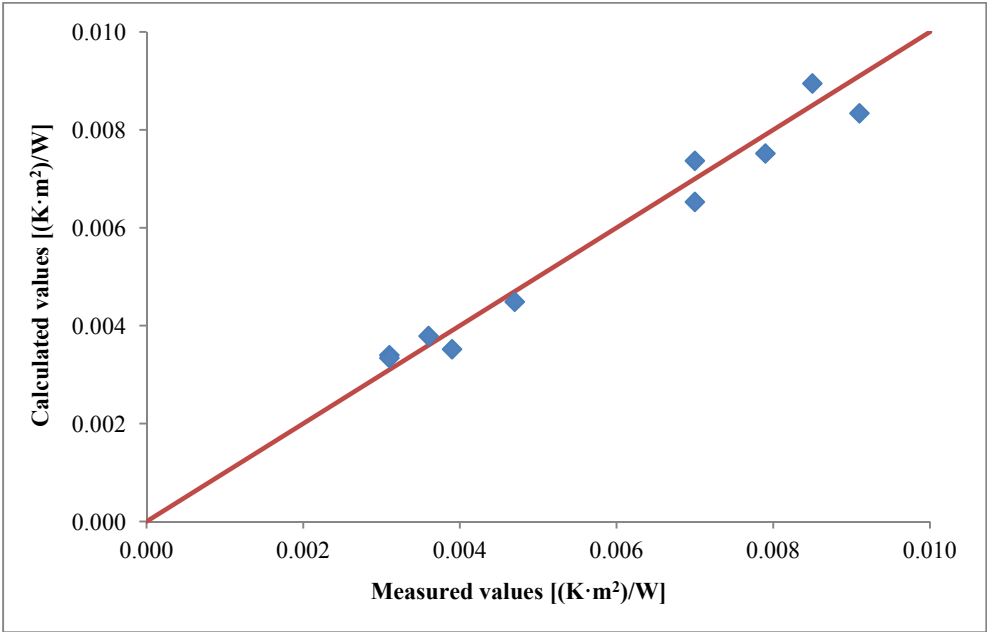
Figure 4.25 - Parity plot for thermal resistance values

As it can be seen, there is a quite good agreement between the literature data and the simulations results, with a maximum error of about 10%.

Differing from air permeability simulations for thermal resistance values the error between literature and simulated values is higher; this is probably due to the simplification of the real geometry of the fabrics.

These results confirms that thermal resistance of different woven fabrics can be predicted with quite good accuracy using only the basic design parameters of any fabric and using a simplified geometry.

4.4.2 - Simulation of thermal resistance of a fabric on a human body

When garments are worn on a human body there are some contact point between fabric and skin but there are also some areas where the fabrics is far from the skin; these situations are quite different from the measurements that can be done using ALAMBETA instrument, due to the presence of a thin layer of still air trapped between fabric and skin and to the absence of any flattening.

A scheme of the real situation is shown in Fig. 4.26.
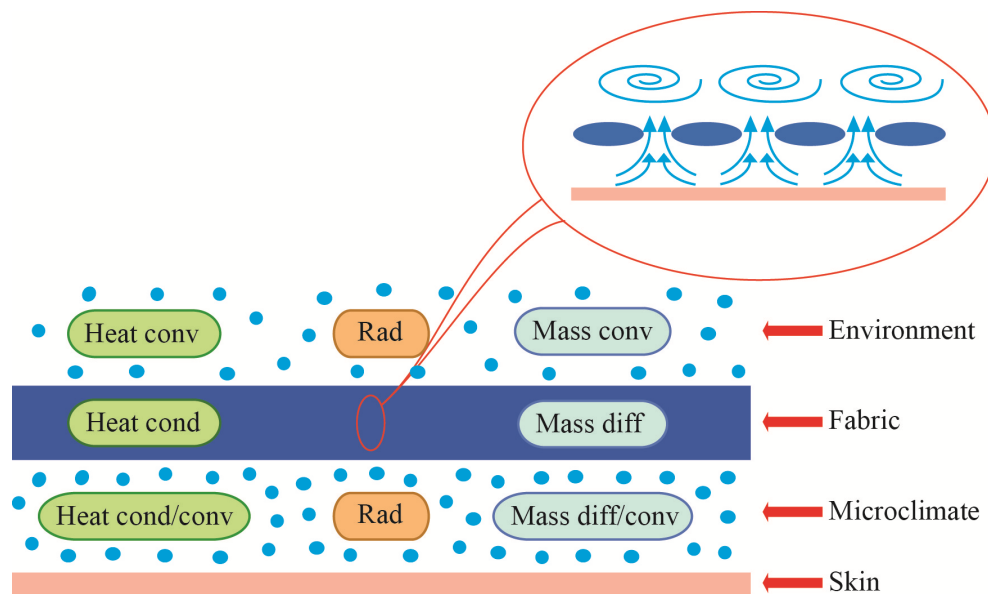
Figure 4.26 - Heat and mass mechanisms in the real case

In order to analyze what happens when the fabrics distance from the skin vary from contact to 5 mm, some 2D simulations has been done; two different 2D model has been derived from a 3D geometry, the first as section done in the middle of a yarn and the second as section done between two yarns, as shown in Fig. 4.27.
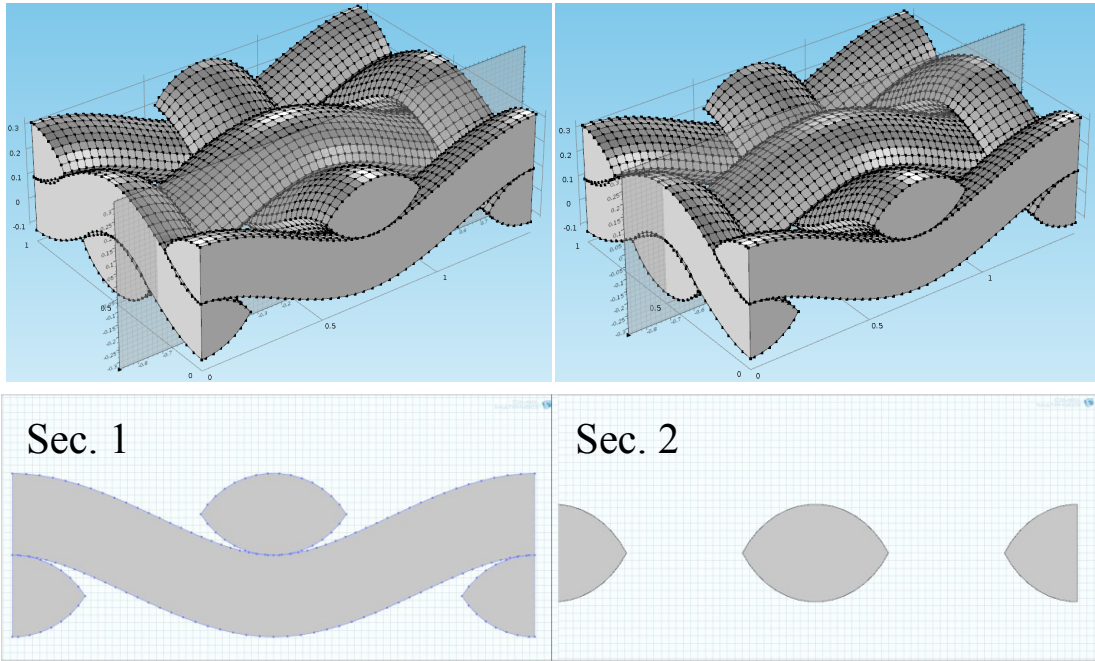
Figure 4.27 - Fabric sections used for simulations

Two different physics interfaces have been used into COMSOL in order to analyze these two geometries, namely free and porous media flow, already described for air permeability simulations, coupled with the heat transfer in porous media used also for thermal resistance. In this way it is possible to analyze the effect of the fabric structure (macro and micro pores) combined with the distance from the skin surface, taking into account the convective vortex due to natural convection.

The skin temperature has been set at 32 °C while the temperature of the environment has been set at 20 °C; an air flow velocity of 0.1 m/s has been also considered.

In Fig. 4.28 are reported the boundary conditions used for simulations.
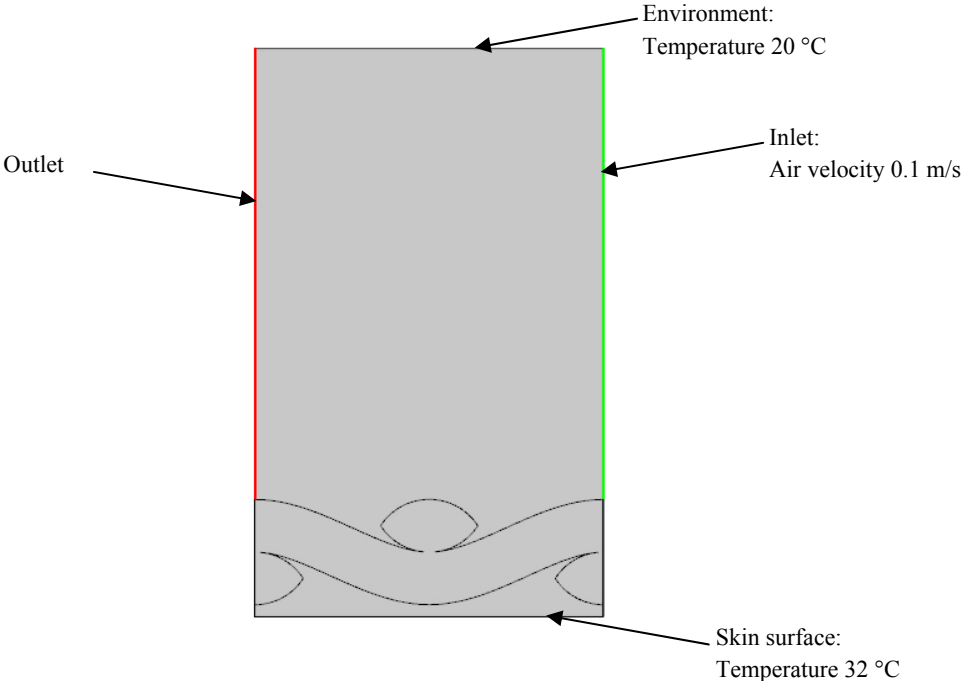
Figure 4.28 - Boundary conditions used in simulations

At the environment boundary not only temperature but also open boundary condition has been set.

A non slip condition has been set at the outer fabric surface.

The results of the simulations, in terms of heat flux, are reported in Fig. 4.29.
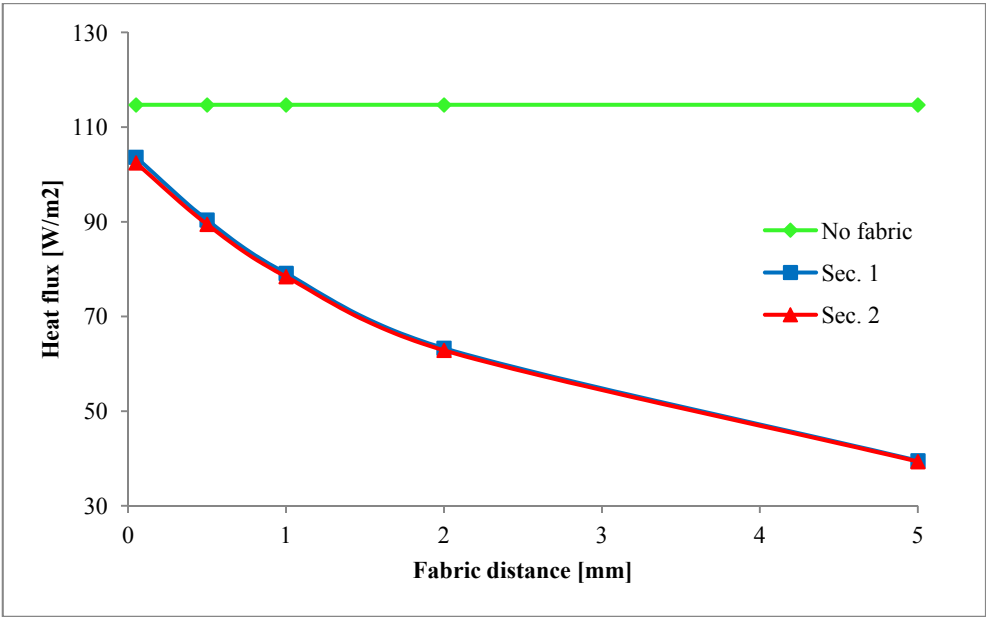
Figure 4.29 - Heat flux at different fabric distances from the skin

As it can be seen the heat flux in case of clothed condition is lower than for a naked body; for a clothed condition the heat flux depends mainly from the fabric distance from the skin surface and there is a very little difference between section 1 and section 2.

In order to better simulate the real condition of a clothed body some simulations has been carried out considering the Fanger model for thermal comfort [3]; in these cases the internal heat production has been set in COMSOL at the skin surface and the heat exchange terms due to respiration, water diffusion and sweat evaporation calculated using the following equations.

$$E_d = 3.05 \cdot \left[5.73 - 0.007 \cdot (M - W) - P_a \cdot 10^{-3} \right] \qquad [4.45]$$

$$E_{sw} = 0.42 \cdot \left[(M - W) - 58.15 \right] \qquad [4.46]$$

$$E_{re} = 1.72 \cdot 10^{-5} \cdot M \cdot \left[5867 - P_a \right] \qquad [4.47]$$

$$L = 0.0014 \cdot M \cdot (34 - t_a) \qquad [4.48]$$

where:
E_d: heat loss by water vapour diffusion through skin [W/m^2]
E_{sw}: heat loss by evaporation of sweat from skin surface [W/m^2]
E_{re}: latent respiration heat loss [W/m^2]
L: dry respiration heat loss [W/m^2]
H: internal heat production [W/m^2]
M: metabolic rate [W/m^2]
W: external work [W/m^2]
P_a: partial pressure of air [Pa]
t_a: air temperature [°C]

Boundary conditions for inlet, outlet and environment are the same used in the previous case.

In the following figures simulations results are reported for the two different metabolic heat production, namely 100 W/m^2 and 150 W/m^2.
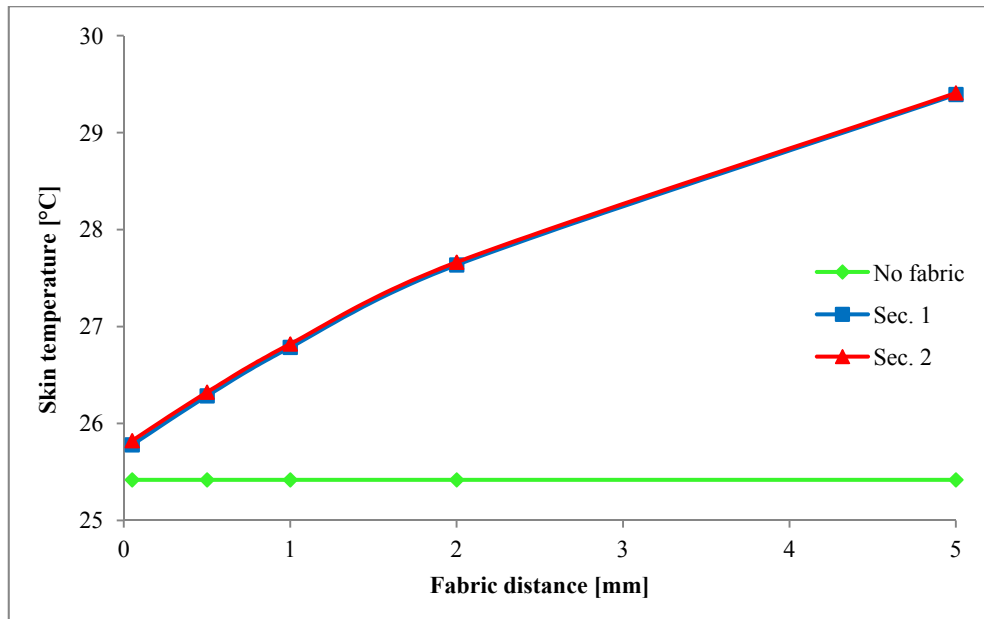
Figure 4.30 - Skin temperature with a metabolic heat production of 100 W/m^2
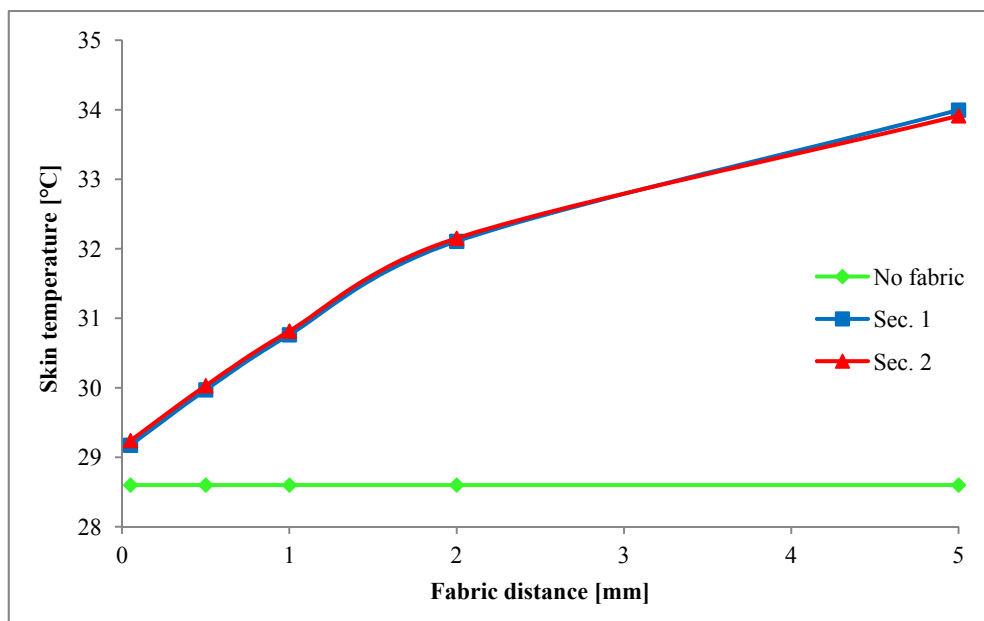
Figure 4.31 - Skin temperature with a metabolic heat production of 150 W/m^2

As it can be seen from simulation results, fabric distance from the skin surface has a great influence on the thermal properties, due to the air layer trapped between skin and fabric. Also the heat flux, that depends on the metabolic heat production and external work, has a great influence on the skin temperature and consequently on the condition of comfort.

4.5 - Water vapour transport and moisture adsorption

The third main characteristic that has been investigated is the moisture adsorption and the vapour transport properties of a fabric. In fact, vapour produced by perspiratio insensibilis is not only transported through the fabric to their surface but it is also adsorbed by the fibres.

Adsorption process is highly dependent from the fibre material where natural fibres can reach high regain than synthetic fibres and from the ambient temperature; as example regain as function of relative humidity, for different fibres materials, is reported in Fig. 4.32 [16].
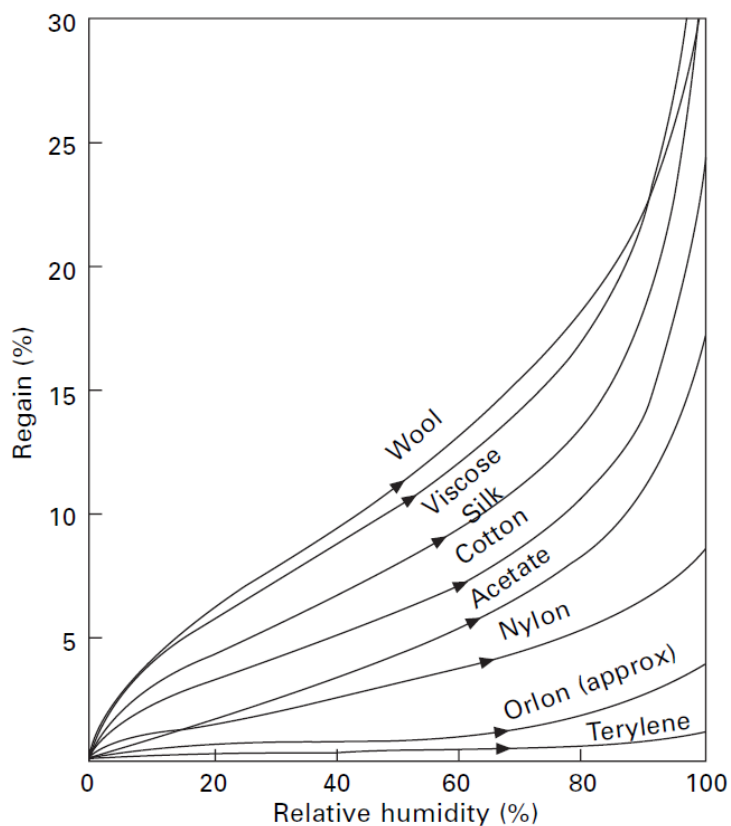
Figure 4.32 - Regain versus relative humidity for different fibres at 25°C

In order to analyze the adsorption process for different fibre material, some simulation has been done using COMSOL Multiphysics®.

The geometrical model of a yarn section, calculated using the Hearle model described in Chap. 2, has been created directly into COMSOL, as shown in Fig. 4.33.
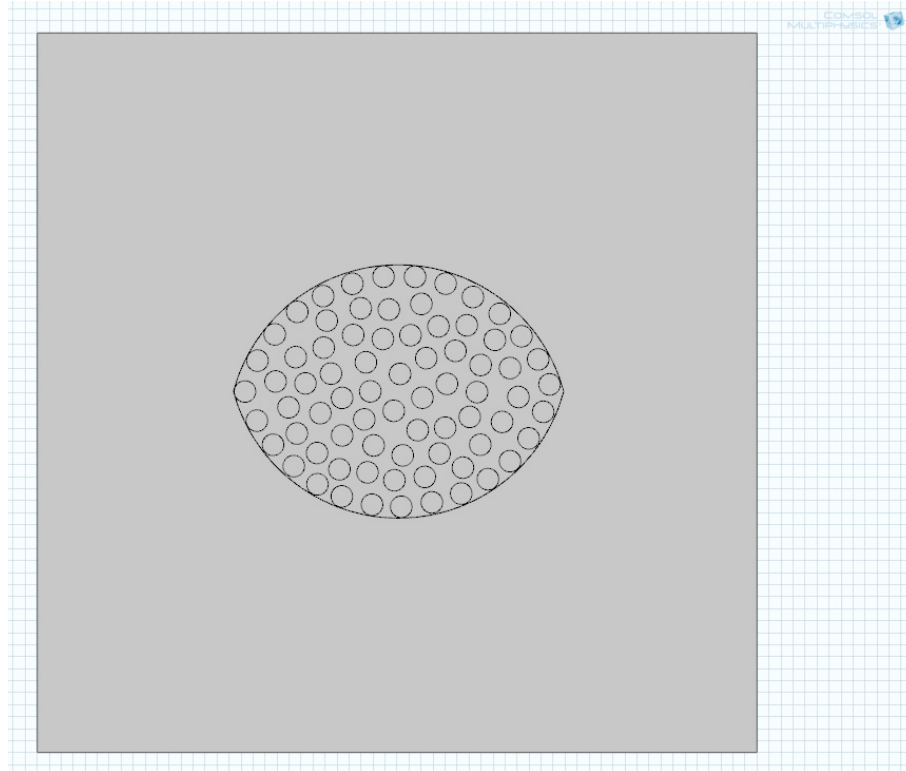
Figure 4.33 - 2D model of a yarn section

In order to simulate the transport of water vapour inside the yarn and then the adsorption process, two different physical interface have been set into COMSOL:
- ➢ The Transport of Diluted Species, to analyze the transport of water vapour inside the yarn
- ➢ The ODE interface, to set up the adsorption process using an ordinary differential equation

In the free volume the diffusion coefficient has been defined using the equation proposed by Boca [58]:

$$D_f = -2.775 \cdot 10^{-6} + 4.479 \cdot 10^{-8} * T + 1.656 \cdot 10^{-10} * T^2 \qquad [4.49]$$

where
D_f : diffusion coefficient [m²/s]
T: air temperature [K]

In the fibres domain an effective diffusion coefficient has been calculated from Eq. 4.50.

$$D_e = \frac{D_f \cdot \varepsilon}{\tau} \qquad [4.50]$$

where
D_e : effective diffusion coefficient [m^2/s]
D_f : diffusion coefficient [m^2/s]
ε: fibre porosity
τ: fibre tortuosity

As boundary condition, a constant concentration of water in air has been set that means that the air humidity can be considered as constant in time;

In the free volume the Fick's law (Eq. 4.51) has been used to simulate the water vapour transport while in the porous domain the Fick's law has been modified in order to take into account both the porosity and the adsorption process (Eq. 4.52).

$$\frac{\partial C_i}{\partial t} + \nabla \cdot \left(-D_f \nabla C_i \right) = 0 \qquad [4.51]$$

$$\left(\varepsilon + \rho_b k_{p,i} \right) \frac{\partial C_i}{\partial t} + \left(C_i - C_{p,i} \rho_p \right) \frac{\partial \varepsilon}{\partial t} = \nabla \cdot \left(D_e \nabla C_i \right) \qquad [4.52]$$

where
D_e : effective diffusion coefficient [m^2/s]
D_f : diffusion coefficient [m^2/s]
C_i: water content in the air [moles/m^3]
ε: fibre porosity
ρ_b: bulk density [kg/m^3]
$k_{p,i}$: adsorption isotherm
$C_{p,i}$: amount of water adsorbed to the solid matrix [moles/kg]

The amount of water adsorbed to the solid matrix can be expressed, using the adsorption isotherm, as function of the water content.

$$C_{p,i} = k_{p,i} \cdot C_i \qquad [4.53]$$

In the porous domain, the ODE interface has been used to define the adsorption isotherms for the different fibres; wool and nylon isotherms at 25°C are reported in Eq. 4.54 [59] and Eq. 4.55 [60].

$$R\% = 3 \cdot 10^{-8} \cdot RH^5 - 7 \cdot 10^{-6} \cdot RH^4 + 6 \cdot 10^{-4} \cdot RH^3 - 0.025 \cdot RH^2 + 0.6119 \cdot RH \qquad [4.54]$$

$$R\% = 7 \cdot 10^{-9} \cdot RH^5 - 2 \cdot 10^{-6} \cdot RH^4 + 2 \cdot 10^{-4} \cdot RH^3 - 0.0062 \cdot RH^2 + 0.1531 \cdot RH \qquad [4.55]$$

where
$R\%$: regain (%)
RH: relative humidity (%)

The simulations results for wool and nylon fibres, with an air temperature of 25°C and a relative humidity of 55%, are shown in Fig. 4.34.
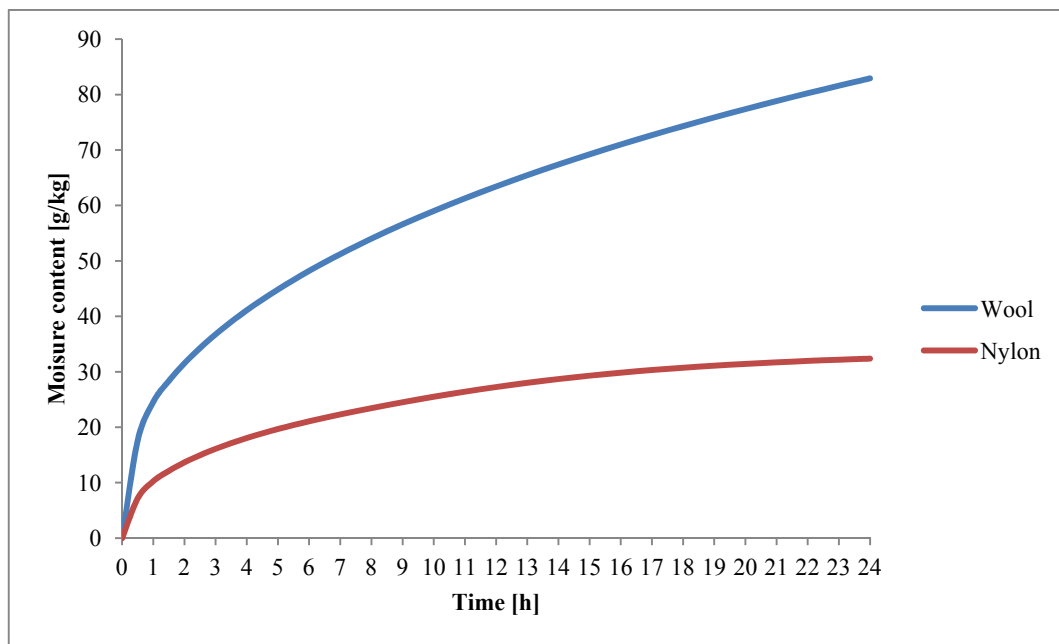
Figure 4.34 - Adsorption of water vapour for wool and nylon fibres at 25°C and 55 RH%

As it can be seen adsorption is a slow process that has no influence for comfort evaluation of garments used during high intensities physical activities; this is due to the rapidly increase of the humidity in the air layer trapped between the skin and the fabric to the saturation value. In this case, due to the presence of liquid water, the transport of liquid prevail on the vapour transport.

Adsorption has to be considered for low intensities physical activities where the air layer can reach a temperature of about 30°C-40°C and a relative humidity of about 60%-90%; in this case the adsorption of vapour should be taken into account together with the vapour transport through the fabric.

As example, simulations results for wool fibres at different relative humidity and temperature values, is reported in Fig. 4.35, Fig. 4.36 and Fig. 4.37.
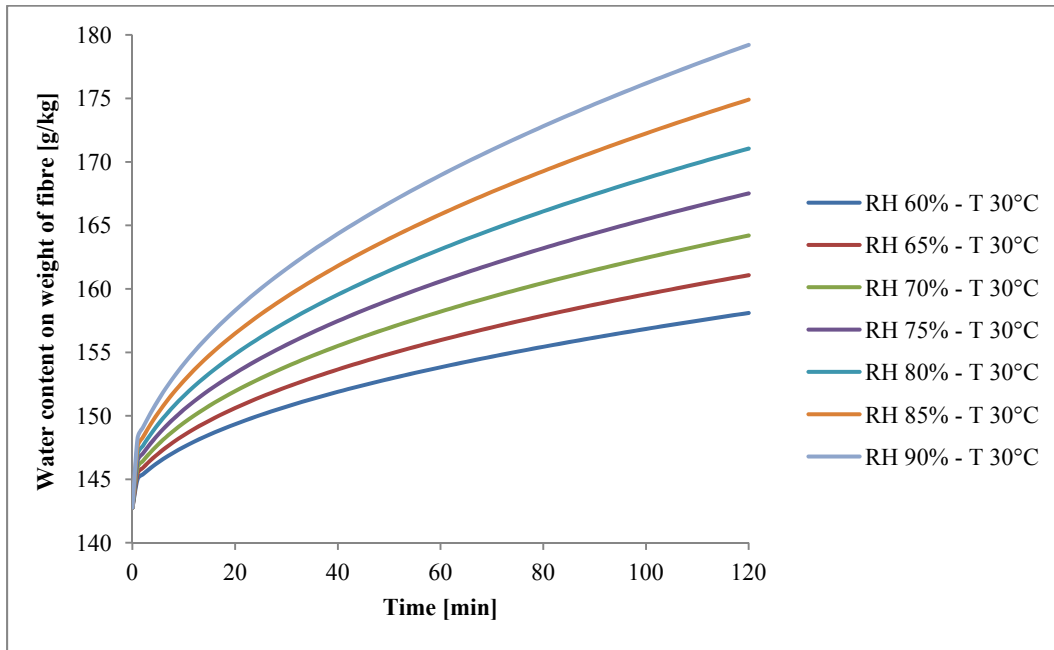

Figure 4.35 - Moisture content at different relative humidity values at 30 °C
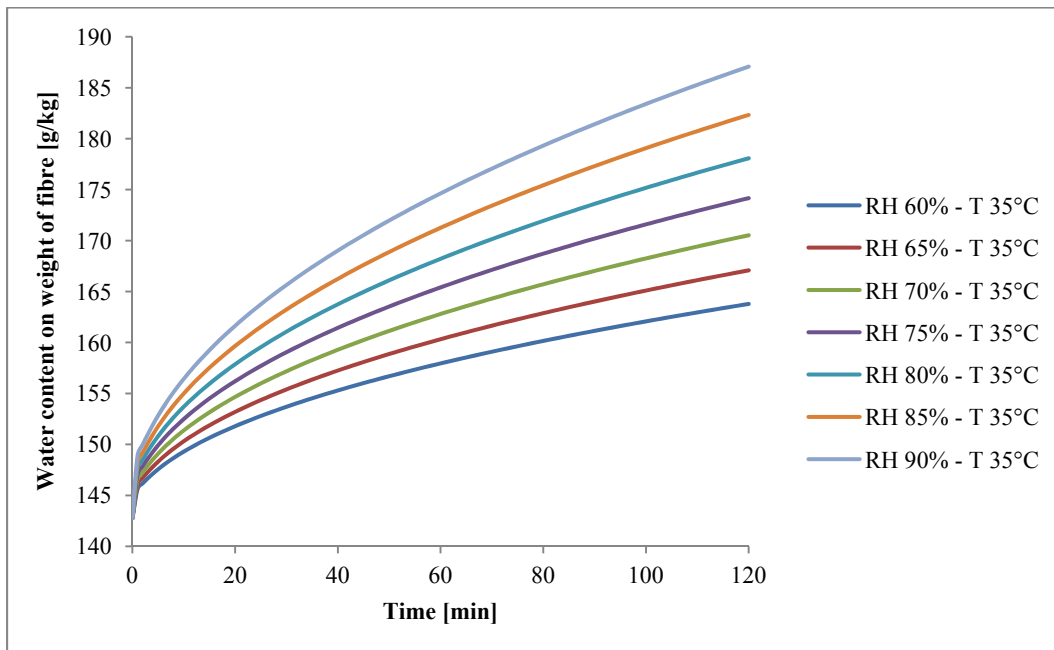
Figure 4.36 - Moisture content at different relative humidity values at 35 °C
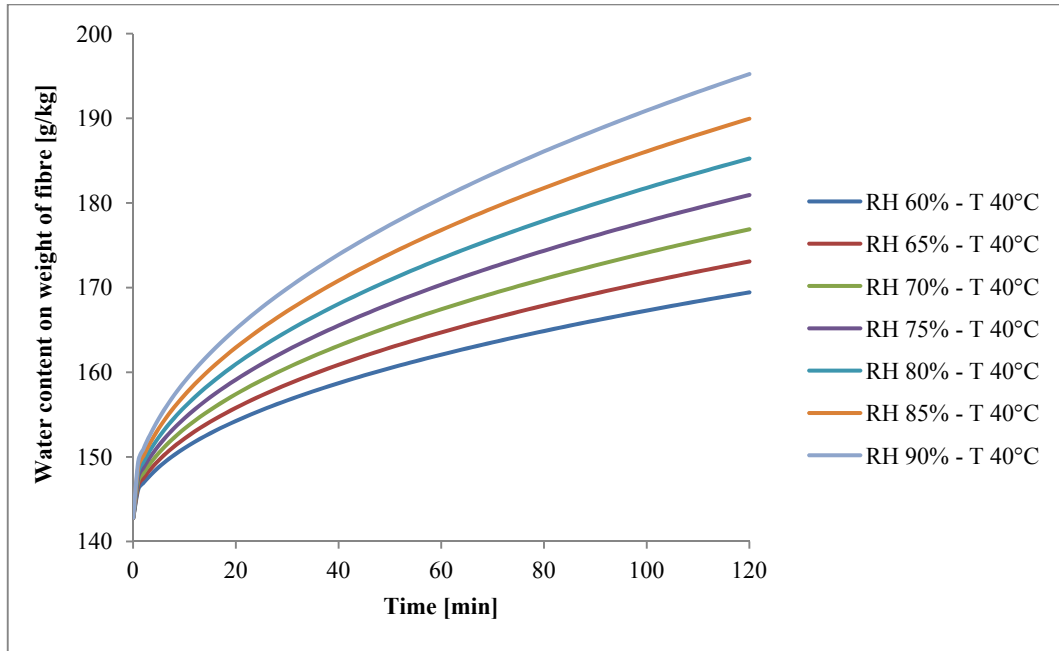
Figure 4.37 - Moisture content at different relative humidity values at 40 °C

Considering that adsorption is an exothermic process, using the adsorption model it is possible to predict the heat generated from the different fibres due to the moisture adsorption.

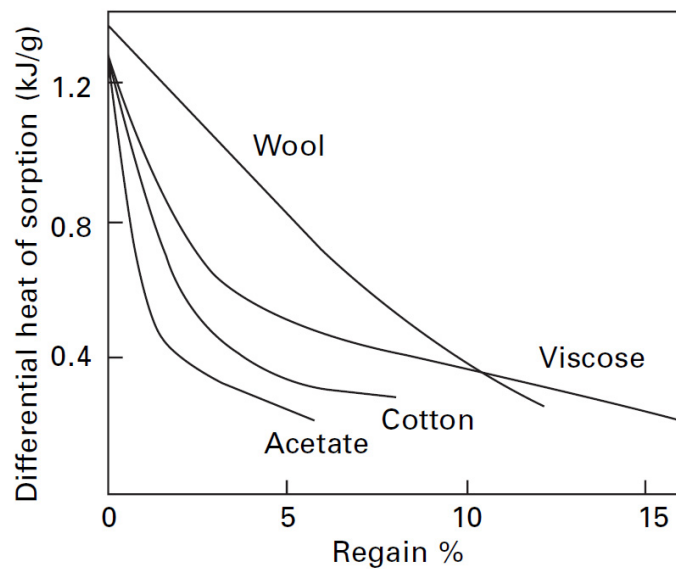As example the differential heat of sorption for different fibres is reported in Fig. 4.38 [16].

Figure 4.38 - Differential heat of sorption for different fibres [16]

5 - Case study: back protectors

5.1 - Introduction

Back protectors are very useful in order to avoid injuries of the back especially for all the sports that usually consider strong impacts such as motorsport, ski, etc...; they shield the spinal cord and protect from injuries, such as the paralysis of the lower part of the body.

In the last years some innovations have been done for back protectors production and classical hard-shell protectors, composed from a shell of thermoplastic material combined with a soft foam layer, have been replaced by soft-shell back protectors composed by soft polymeric foams; in fact, it is important to consider that the safest back protector is the one that is wear more often and to reach this goal it is necessary that back protector is very comfortable both in terms of thermo-physiological comfort and freedom of movements.

These soft polymeric foams present a pseudo-dilatants behaviour, reacting like a soft and viscous material when they are under low mechanical stresses and like a rigid material when they are hit with high shear stresses.

5.2 - Experimental data

One back protector has been tested in a climatic room at Laboratories of Advanced Textile Technology in Biella; it is shown in Fig. 5.1.

Marker Body Vest

Figure 5.1 - Back protectors

Its properties are reported in Tab. 5.1.

Type	Chemical composition	Mass [g]	Density [g/cm^3]	Thickness [mm]
Marker	EVA and nitrile rubber	345	0.15	16

Table 5.1 - Back protector characteristics

The back protector is built from a layer of protection material encapsulated between textile layers, whose properties are reported in Tab. 5.2.

Type	Textile composition	Weight [g]
Marker	80% Polyammide 20% Elastan	685

Table 5.2 - Textile layers characteristics

Five testers, two men and three women, have been selected for the in-vivo tests and all testers were wearing identical clothes, namely long sleeved vest and long pants, as shown in Fig. 5.2.

Figure 5.2 - Testers underwear

All tests have been carried out at temperature of 12°C and relative humidity of 65% and consists in a series of three different phases made on a treadmill:

➢ Acclimation phase: at rest for 10 minutes
➢ Activity phase: 20 minutes with four intensity peak from 5 km/h to 10 km/h every 5 minutes
➢ Cooling phase: at rest for 30 minutes

For every tester temperature and relative humidity of the air layer between the skin and the underwear have been monitored using 11 sensors, placed as shown in Fig. 5.3.

Forehead
Right scapula/left scapula
Right chest/ Left chest
Right deltoid
Left elbow
Left back hand
Right thigh
Left calf
Lower back, center
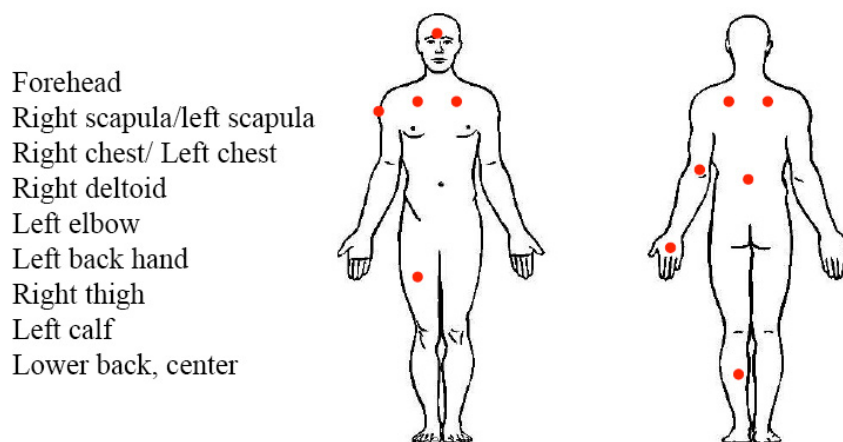
Figure 5.3 - Sensors displacement

In addition to sensors measurements also a high resolution thermographic camera has been used; at the end of each step thermographic images of the volunteers back were acquired.

As example, temperature, relative humidity of the microclimate on the back and heart rate of one of the tester are reported in Fig. 5.4, Fig. 5.5 and Fig. 5.6.
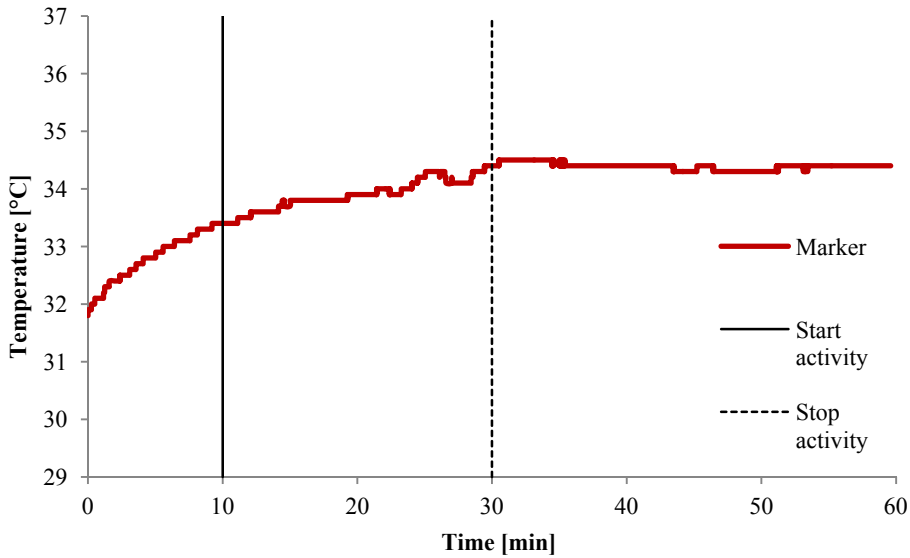
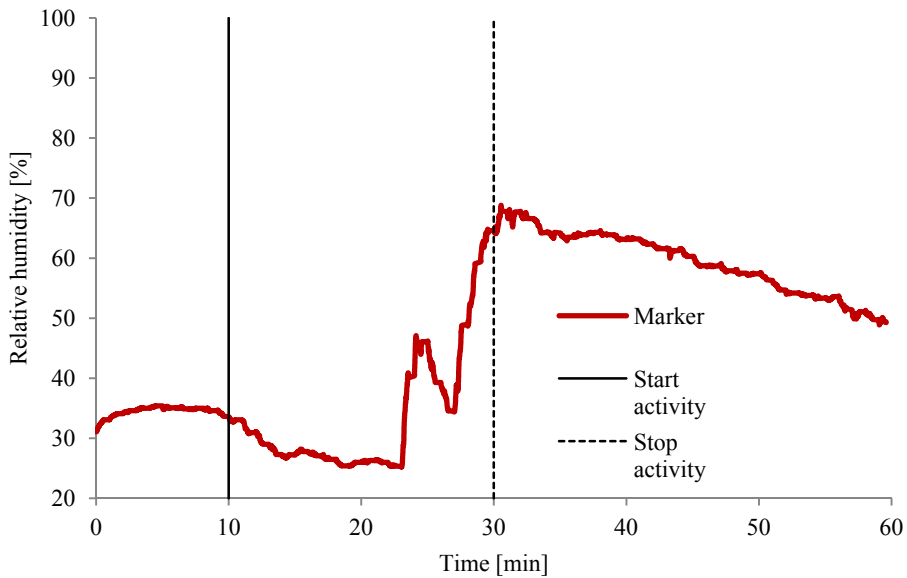

Figure 5.4 - Temperature of the microclimate

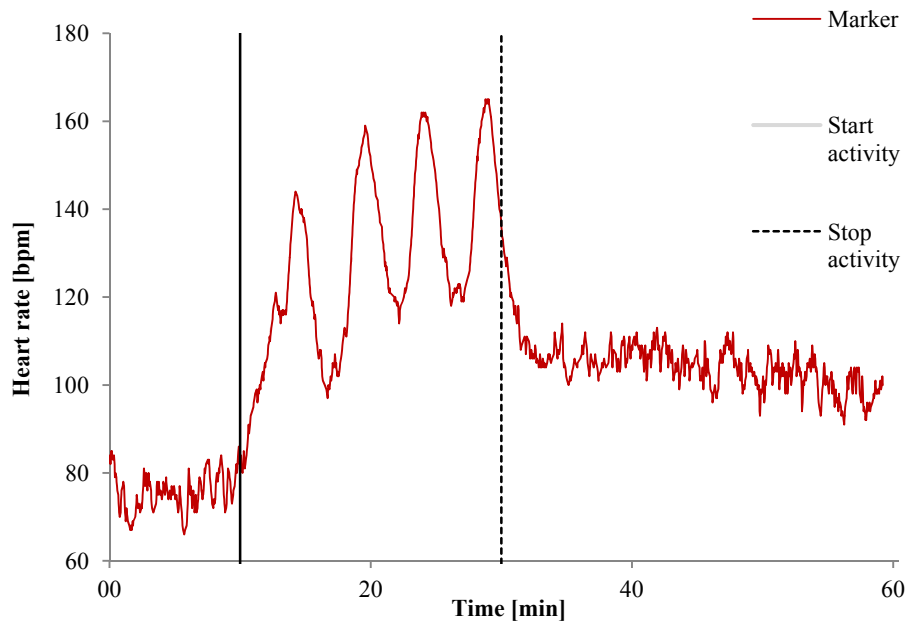Figure 5.5 - Relative humidity of the microclimate

Figure 5.6 - Heart rate

Fig. 5.4 shows that the temperature of the air layer increase from about 31°C to 35°C and remain approximately constant also during the resting phase. On the contrary from Fig. 5.5 it is possible to see that relative humidity in the microclimate increases from about 30% to 70% but starting during the activity phase; this can be correlated to the mechanism of thermoregulation of the human body where the heat generated is first released with an increase in the skin temperature and then using sweat that remove heat with evaporation.

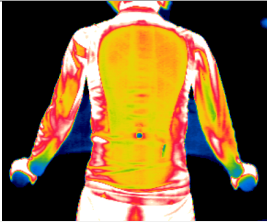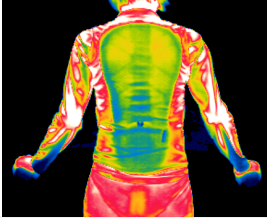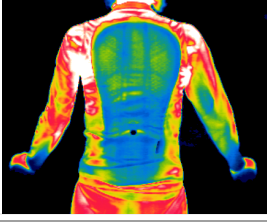In table 5.3 the thermographic images obtained from thermocamera are reported.

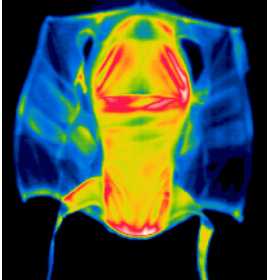| Time [min]	MARKER
10	
30	
45	
60	
60 Inner surface back protector	

Table 5.3 - Thermographic results

5.3 - Simulation with COMSOL Multiphysics®

In order to simulate the behaviour of the back protector, a 3D geometry has been created starting from some photography imported into AutoCAD; the resulting 3D model is shown in Fig. 5.7.
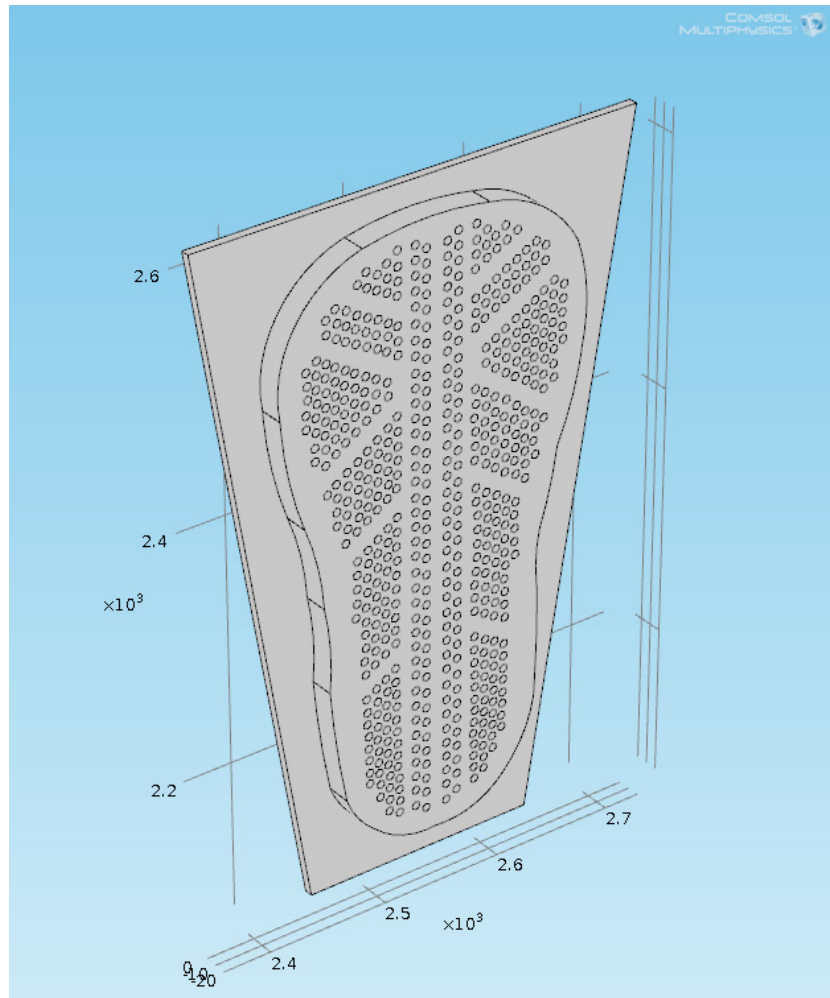

Figure 5.7 - Marker back protector 3D model

As it can be seen from Fig. 5.7 not only the back protector but also the air layer between its inner surface and the skin has been modelled.
For both solid and fluids domains the following heat equation has been used; in the fluid domain the velocity field due to natural convection has been neglected.

$$\rho C_p \frac{\partial T}{\partial t} = \nabla \cdot \left(k \nabla T \right) \qquad [5.1]$$
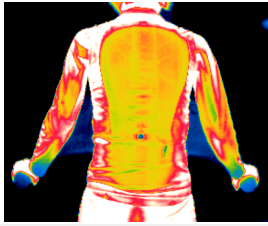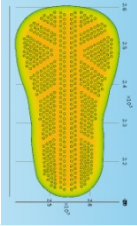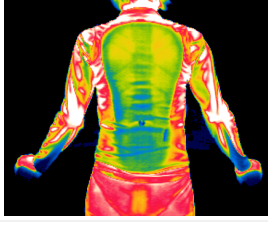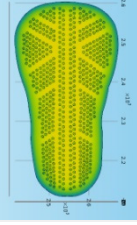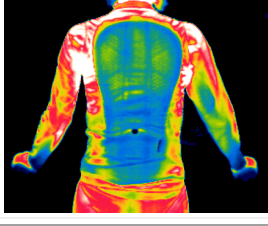
where
ρ: density [kg/m^3]
C_p: specific heat [J/kg·K]
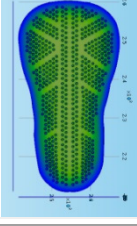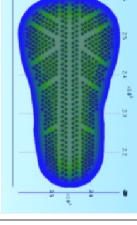
k: thermal conductivity [W/m·K]
T: temperature [K]

Temperature at the skin surface has been set using the experimental data reported in Fig. 5.4 and the heat exchange with the environment has been considered using an heat transfer coefficient of 8 W/m·K and a temperature of 12.8 °C.

In order to compare experimental data recorded using the thermocamera and the simulation values, the colour table of the thermocamera has been imported into COMSOL.

In table 5.4 the simulations results compared with the experimental thermographic images are reported.

Time [min]	Experimental data	Mean temperature [°C]	Simulation data	Mean temperature [°C]
10		19.40		19.10
30		18.00		17.80
45		17.15		17.40
60		17.00		17.25

Table 5.4 - Simulations and experimental results

As it can be seen there is a quite good approximation between the simulation results and the thermographic images confirmed also from the mean temperature values; it is possible to conclude that using modelling techniques it is possible to predict not only the comfort properties of fabrics but also garments behaviour under different physical activities intensities and environmental conditions.

6 - Conclusions

The first part of this work has allow to analyze the mechanisms that mainly affect the thermo-physiological comfort; it is a subjective complex feeling influenced from clothing properties, environmental conditions and physical activity. Nevertheless it is necessary to study comfort under an objective point of view in order to evaluate a subjective feeling using some objective tests.

This research has been focused on the relationship between fabrics properties and the connected comfort behaviour; because fabric has a complex 3D structure composed from yarns and fibres a great attention has been paid on the geometrical modelling of the fabric structure in order to obtain more accurate simulation data.

Starting from the basic design parameters of yarns and fabrics and using the geometrical fabric model developed by Hearle, all the fabrics geometrical parameters have been defined; later, using TexGen, an open source software developed at the University of Nottingham in 1998, the fabric geometries have been created and then imported into COMSOL Multhiphysics®, a finite element method simulation software, in order to predict their comfort properties.

Three main comfort properties, namely air permeability, thermal resistance and vapour adsorption have been taken into account and for each one suitable simulations have been carried out.

The air permeability simulations, carried out for ten different fabrics, have shown good agreements with experimental values found in literature.

Thermal resistance properties have been studied under two different point of view.

First, ten different fabrics have been created and their simulations results compared to experimental data found in literature; starting from the real 3D geometry created as for air permeability analysis, a simplified geometry has been derived in order to better represents the experimental tests. Using these simplified geometries a quite good approximation has been obtained.

In the second case the heat transfer through a fabric place at different distances from the skin surface has been analyzed; two different boundary conditions, namely constant temperature and constant heat flux, have been considered. Simulations results show that the presence of the fabric and its distance from the skin surface are the most important parameters that influence the heat transfer; simulations show that there are also an influence due to the presence of macro-pores.

Also moisture adsorption has been investigated for different fibres materials and air temperature and humidity conditions; from the simulations results it is possible to conclude that adsorption process, that is negligible under high intensity physical activities, has to be considered in order to take into account heat generated from this process.

Finally a case study, a back protector garment, has been studied.

Some experimental tests have been carried out in a climatic room at the Laboratories of Advanced Textile Technology in Biella; during these tests, carried out with a treadmill under controlled physical intensities, temperature and humidity in the air layer trapped between the skin surface and the garment surface have been recorded and, using a thermocamera, also the temperature of the outer back protector surface has been measured. For simulation purposes, a 3D model of a back protector has been created and using experimental data some simulations have been carried out in order to model the garment behaviour. Simulation results show good approximation with experimental ones obtained from the thermocamera.

This research work shows that using modelling techniques it is possible to predict with quite good approximation the comfort properties of any woven fabrics starting from its design parameters. Also comfort behaviour of garments can be predicted under different environmental conditions and physical activity intensities.

This simulation method allow to reduce the costs for the development of new high performance fabrics.

Bibliography

[1] K.L. Hatch, Textile science, West Publishing Co., Minneapolis, 1993, p.26.

[2] K. Slater, Human comfort, Charles C. Thomas Publisher, Springfield, 1985, p.4.

[3] K. Parson, Human thermal environments, 2°ed., Taylor & Francis, London, 2003.

[4] D.A. McIntyre, Indoor climate, Elsevier, London, 1980.

[5] W.R. Santee, R.R. Gonzalez, Characteristics of the thermal environment, in K.B. Pandolf, M.N. Sawka, R.R. Gonzalez, Human performance physiology and environmental medicine and terrestrial extremes, Brown & Benchmark Pub, USA, 1988.

[6] K.B. Pandolf, M.N. Sawka, R.R. Gonzalez, Human performance physiology and environmental medicine and terrestrial extremes, Brown & Benchmark Pub, USA, 1988.

[7] D. DuBois, E.F. DuBois, A formula to estimate surface area if height and weight are known, Archive of internal medicine, v. 17, 1916, p. 863.

[8] P.O. Fanger, Thermal comfort, Danish Technical Press, Copenhagen, 1970.

[9] P. Astrand, K. Rodahl, Textbook of work physiology-physiological bases of exercise, 3° ed., McGraw-Hill, New York, 1986.

[10] P.R.M. Jones, G.M. West, D.H. Harris, J.D. Read, The loughborough anthropometric shadow scanner (LASS), Endeavour, v.13, 1989, pp.162-168

[11] E.A. McCullough, B.W. Jones, A comprehensive database for estimating clothing insulation, IER Technical Report, Kansas State University, v.84-01, 1984.

[12] K.C. Parsons, Protective clothing: heat exchange and physiological objectives, Ergonomics, v.31, 1988, pp. 991-1007.

[13] D.M. Kerslake, The stress of hot environment, Cambridge University Press, Cambridge, 1972.

[14] W.A. Lotens, Comparison of the thermal predictive models for clothed humans, ASHRAE Transactions, v.94, 1988.

[15] W.A. Lotens, Clothing thermal evaluation using heat balance techniques, Proceedings of the international conference on environmental ergonomics, Austin, 1990.

[16] W.E. Morton, J.W.S. Hearle, Physical properties of textile fibres, 4°ed, Woodhead publishing, Cambridge, 2008.

[17] M. Bona, F.A. Isnardi, S.L. Straneo, Manuale di Tecnologia Tessile, Zanichelli, Roma, 1981.

[18] C. Mazza, P. Zonda, Quaderni di Tecnologia Tessile: la maglieria, Fondazione ACIMIT, Milano, 2003.

[19] G. Tanchis, Quaderni di Tecnologia Tessile: i nontessuti, Fondazione ACIMIT, Milano, 2008.

[20] K. Slater, Comfort properties of textiles, Textile Progress, v.9, 1977.

[21] W.H. Rees, Physical factors determining the comfort performance of textiles, Third Shirley International Seminar, Manchester, 1971.

[22] W. Runbai, Y. Hang, The measures of clothing insulation using a heated manikin, Proceedings of the 11th Congress of the International Ergonomics Association, Paris, 1991, pp. 1146-1148.

[23] H. Meinander, Heat stress in sportswear, assessment of heat and moisture transmission, Proceedings of International Conference of Textiles in Sports and sportswear, Huddersfield, 1995, pp. 46-52.

[24] V. Kondratskii, Izv. Vyssh. Uchebn. Zaved., Tekhnol. Tekst. Prom., v.4, 1972.

[25] G. Alibert, Industrie Textile, 1972, p.919.

[26] E. Köhler, S. Pietsch, Textiltechnik, v.23, 1973, p. 640.

[27] V.K. Kothari, A. Newton, The air permeability of nonwoven fabrics, Journal of the Textile Institute, v.65, 1974, pp.525-531.

[28] M. Havlovà, Air Permeability and Constructional Parameters of Woven Fabrics, Fibres & Textiles in Eastern Europe, v.21, 2013, pp.84-89.

[29] I. Fatahi, A.A. Yazdi, Predicting Air Permeability from the Parameters of Weave Structure, Fibres & Textiles in Eastern Europe, v.20, 2012, pp.78-81.

[30] R.T. Ogulata, S. Mavruz, Investigation of Porosity and Air Permeability Values of Plain Knitted Fabrics, Fibres & Textiles in Eastern Europe, v.18, 2010, pp.71-75.

[31] K. Yazdchi, S. Srivastava, S. Luding, Microstructural effects on the permeability of periodic fibrous porous media, International Journal of Multiphase Flow, v.37, 2011, pp.956–966.

[32] Q.Wang, B. Mazé, H. Vahedi Tafreshi, B. Pourdeyhimi, Anote on permeability simulation of multifilamentwoven fabrics, Chemical Engineering Science, v.61, 2006, pp.8085 – 8088.

[33] UNI EN ISO 9237, Determination of permeability of fabrics to air, 1997.

[34] R.P. Clark, The Aerodynamics of Warmth and Cleanliness, Clothing Research Journal, v.2, 1974, pp.55-67.

[35] H.W. Hackenberg, Wiss. Zelt. Tech. Univ. Dresden, v.21, 1972, p.1131.

[36] V.I. Yankelevich, Heat Transfer Through Air-Permeable Materials, Technol. Text. Industr. U.S.S.R., v.1, 1971, p.98.

[37] S. Tilajka, Magyar Textiltech., v.23, 1971, p.426.

[38] L.I. Weiner, J. Shah, Thermal insulation on heat transfer, Text. Chem. Col, v.1, 1969, p.301.

[39] K.V. Karlina, L.I. Tretyakova, Investigation of the effect of macro-layers of air on the thermal insulation properties of clothing assemblies, Tekhnol. Legoi Prom., v.2, 1971, p.98.

[40] G.F. Fonseca, Heat-Transfer Properties of Ten Underwear-Outerwear Ensembles, Textile Research Journal, v.40, 1970, p.553.

[41] L.S. Smirnov, S.S. Zagorodnya, Legka Prom., v.4, 1969, p.47.

[42] UNI EN ISO 5085-1, Determination of thermal resistance, 1989.

[43] L. Hes, J. Williams, Laboratory measurement of thermo-physiological comfort, Improving comfort in clothing, Woodhead Publishing, Cambridge, 2011.

[44] L. Hes, P. Offermann, I. Dvorakova, The Effect of underwear on thermal contact feeling caused by dressing up and wearing of garments, Tecnitex 2001 Autex Conference, 2001, pp. 236-245.

[45] M. Yoneda, S. Kawabata, Analysis of Transient Heat Conduction in Textiles and Its Applications', Part II, Journal of Textile Machinery Society of Japan, v.31, 1983, pp.73-81.

[46] J. Zysman, Industrie Text., 1970, p.359.

[47] D. Gogalla, Dtsch. Textiltech., V.22, 1972, p.696.

[48] L.I. Weiner, Text. Chem. Col., v.2, 1970, p.378.

[49] K.H. Umbach, Physiological tests and evaluation models for the optimization of performance of protective clothing, Environmental Ergonomics, Taylor & Francis, London, 1988, pp.139-161.

[50] L. Hes, Water vapour permeability of wool blended fabrics, International Conference on Textile Science, Liberec, 1993.

[51] J.W.S. Hearle, P. Grosberg, S. Backer, Structural mechanics of fibers, yarns and fabrics, v.1, Wiley-Interscience, USA, 1969.

[52] B.R. Gebart, Permeability of Unidirectional Reinforcements for RTM, Journal of Composite Materials, v.26, 1992, pp. 1100-1133.

[53] F.T. Peirce, The geometry of cloth structure, J. Text. Inst., v.28, 1937, pp.45-96.

[54] A. Kemp, An extension of Pierce cloth geometry to the treatment of noncircular threads, J. Text. Inst., v.49, 1958.

[55] J.W.S. Hearle, W.J. Shanahan, An energy method for calculations in fabric mechanics, Part II: examples of application of the method to woven fabrics, J. Text. Inst., v.69, 1978.

[56] Z. Zupin, A. Hladnik, Krste Dimitrovski, Prediction of one-layer woven fabrics air permeability using porosity parameters, Textile Research Journal, v.82, 2011, pp. 117-128.

[57] D. Bhattacharjee, V.K. Kothari, Heat transfer through woven textiles, International Journal of Heat and Mass Transfer, v.52, 2009.

[58] R.E. Bolz, G.L. Tuve, Handbook of tables for applied Engineering Science, CRC Press, 1976, p. 1166.

[59] J.B. Speakman, Adsorption of water by wool, J. Soc. Chem. Ind, v.49, 1930, pp. 209T-213T.

[60] E.A. Hutton, J. Gartside, The adsorption and desorption of water by nylon at 25°C, J. Text. Ind., v.40, 1949, p. T170.